Published in Marine and Petroleum Geology 16, issue 2, 111-134, 1999
which should be used for any reference to this work

Décollement tectonics in the Jura foreland fold-and-thrust belt

A. Sommaruga*

Institut de Géologie, Université de Neuchâtel, rue Emile Argand 11, CH-2007 Neuchâtel, Switzerland

Abstract

Interpretation of more than 1500 km of industry seismic reflection lines from the Swiss and French Jura Mountains and the western Swiss Molasse Basin demonstrates that the Mesozoic and Cenozoic cover of the Jura fold-and-thrust belt has been deformed over a very weak basal décollement and displaced for many kilometers toward the NW, and that the basement is not involved. A depth to the basement map derived from depth conversion of the seismic lines, shows a rather smooth flat basement dipping 1–3 to the S–SE. The low-amplitude broad folds of the Molasse Basin and the external Plateau Jura are controlled by evaporite pillows or anticlines of Middle Triassic age. The high amplitude folds of the Haute Chaîne Jura, however, are related to NW- or SE-vergent thrusts with at least kilometric dipslip displacement that has doubled the entire Jurassic sequence.

The Plateau Jura evaporite-related folds, located in the foreland, are interpreted as early-stage buckle folds. With further deformation, a fault ramp nucleates and develops into thrust-related folds as observed in the Haute Chaîne. Thus, within the fold-and-thrust belt, deformation increases toward the hinterland. In the Molasse Basin, however, low-amplitude folds represent an early deformation stage which could not develop further owing to the load of the overlying thick Tertiary clastic wedge.

Keywords: Jura belt; Seismic structures; Décollement tectonics; Evaporite- and thrust-related folds

1. Introduction

This research presents the geometry of the cover folds and their relation with the basement within the central Swiss and French Jura and the adjacent Molasse Basin (Figs. 1 and 2). More than 1500 km of industry seismic reflection lines (Fig. 5) add to the surface geological observations accumulated over a century by field geologists. The seismic grid is also constrained by several drill holes. These new data have greatly increased knowledge about the deep structures of the Jura area and have constrained models for the formation of the Alpine foreland and Jura arc. The Mesozoic and Cenozoic cover of the Jura fold-and-thrust belt and the adjacent Molasse Basin have been deformed over a weak basal décollement and displaced by some 20 km and more toward the northwest.

However, the development of the Jura belt is still a matter of debate between two fundamentally different views (Fig. 4): on the one hand, an autochtonous folding of the Jura cover above either basement thrust faults or wrench faults (Aubert, 1945; Pavoni, 1961; Rigassi, 1962;

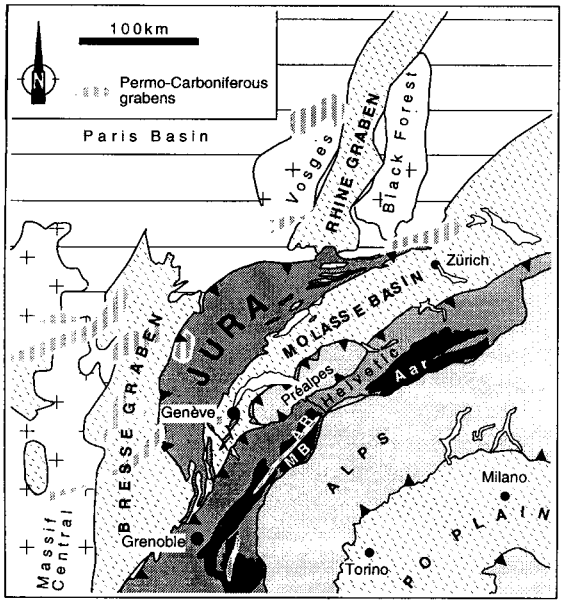

Fig. 1. Location of the Jura arc with respect to the major Cenozoic sedimentary basins (Rhine-Bresse grabens, Molasse Basin, Po Plain) and the Alps. Late Alpine culminations and external crystalline massifs are highlighted in dark gray. AR = Aiguilles Massif; MB = Mont Blanc Massif. Modified from Burkhard and Sommaruga (1998).

* Corresponding author. Tel.: +41-32-718 26 00; fax: 41-32-718 26 01.

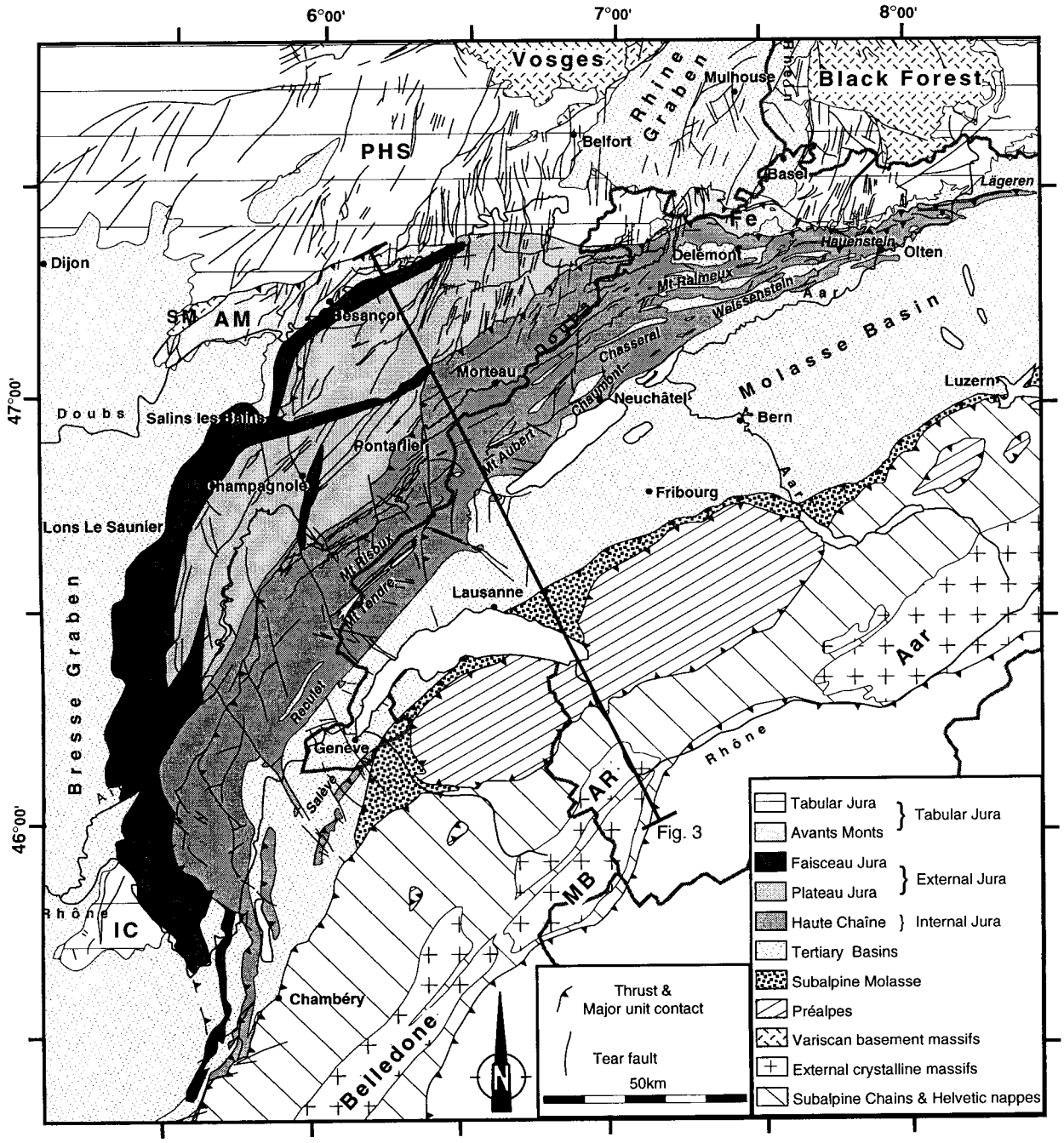

Fig. 2. Tectonic sketch of the Jura arc showing main structural units. Legend: PHS = Plateau de Haute-Saône; IC = Ile Crémieu; AM = Avants-Monts; Fe = Ferrette; AR = Aiguilles Rouges; MB = Mont Blanc. Modified from Sommaruga (1995).

Wegmann, 1963; Ziegler, 1982) and, on the other hand, thin skinned thrusting and associated folding of the Jura cover above a Triassic detachment horizon and displacement over large horizontal distances pushed from the Alps across the Molasse Basin ('Fernschub theory') (Boyer & Elliott, 1982; Buxtorf, 1916; Laubscher, 1973b). Although balancing arguments clearly favor an allochthonous interpretation, seismic data as well as neotectonic arguments have recently been used to support some thick-skinned basement involvement beneath the Jura and the Molasse Basin (Ziegler, 1982; Guellec et al., 1990; Gorin et al., 1993; Pfiffner, 1994; Signer & Gorin, 1995; Pfiffner et al., 1997). For a more complete review on the evolution of the ideas on the formation of the Jura belt, see Sommaruga (1997).

2. Geological setting

The Jura is a small, arcuate fold belt forming the frontal portion of the western Alpine arc (Fig. 1). The Jura

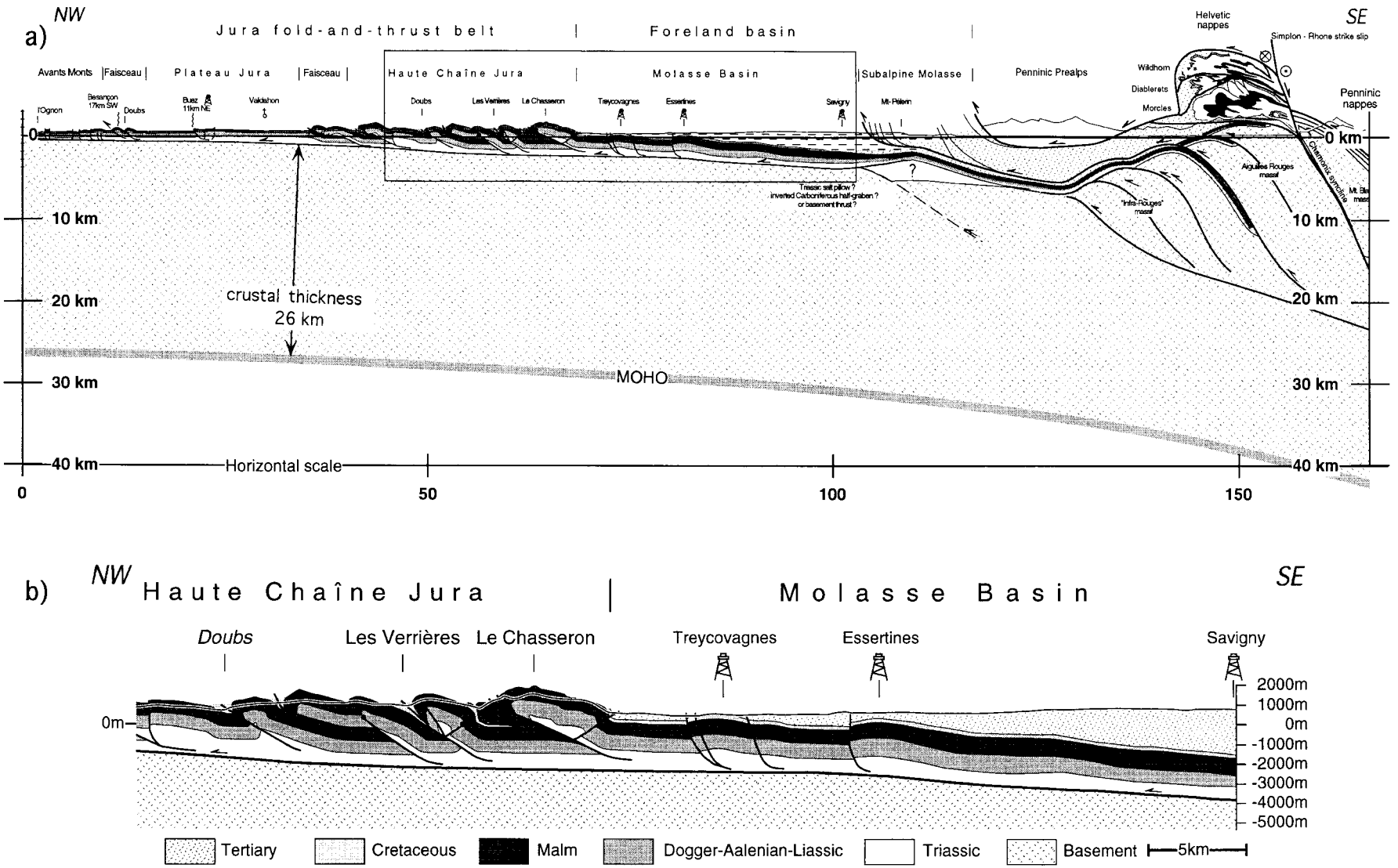

Fig. 3. (a) Large-scale balanced cross-section across the Molasse Basin from the external Jura to the Alps (external crystalline massifs). For location, see Fig. 2. Modified from Burkhard and Sommaruga (1998); (b) Enlargement of the Jura Haute Chaîne–Molasse Basin region from the above large scale cross-section.

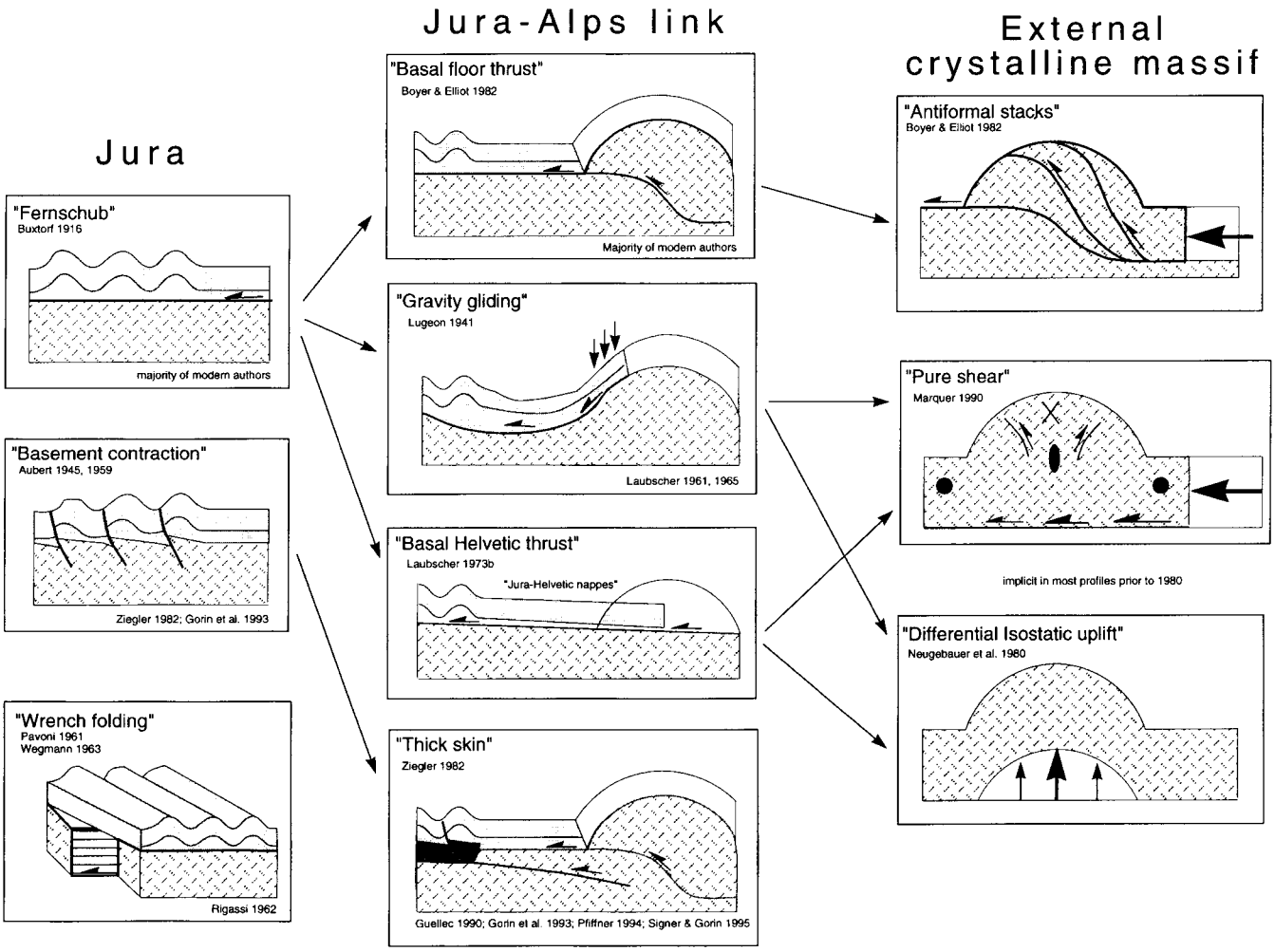

Fig. 4. Conceptual models on the formation of the Jura fold-and-thrust belt and its links to the Alps (external crystalline massifs). Modified from Burkhard (1990).

arc is surrounded by Tertiary basins of different types: to the north, the Rhine Graben; to the west, the Bresse Graben; and to the south-southeast, the Molasse Basin. The Rhine and Bresse Grabens are associated with the Eocene and younger, West-European rift system, whereas the Molasse Basin corresponds to an Oligo-Miocene foredeep, which developed in front of the Alpine orogen. The Jura and the Molasse Basin represent the most external foreland fold-and-thrust belt and the youngest (from Middle Miocene onward) deformation zone of the northwestern Alps. At its southern termination, the Jura belt merges with the Subalpine Chains, which were folded during the same period. Along its western border, the Jura over-thrusts the Bresse Graben, whereas in the north, it overrides the Tabular Jura. At its eastern end, the most remote Jura fold dies out within the Molasse Basin. According to Burkhard (1990) and Laubscher (1992), tectonics of the Jura belt and the Molasse Basin are intimately linked.

2.1. The Jura

The Jura is divided into an external and an internal part (Fig. 2) based on different tectonic styles. The external Jura consists of flat areas, Plateaux, limited to the north and separated from each other by so called Faisceaux, narrow stripes comprising numerous small-scale imbrications and tear faults (Fig. 3a). The internal Jura, also referred to as the Haute Chaîne Jura (Fig. 3b), consists of a well-developed fold train. At a large scale, deformation is characterized by major folds, the trend of which swings through 90° from east to south (Fig. 2). Major tear faults oriented at a high angle to fold axes cut the Haute Chaîne Jura at regular intervals.

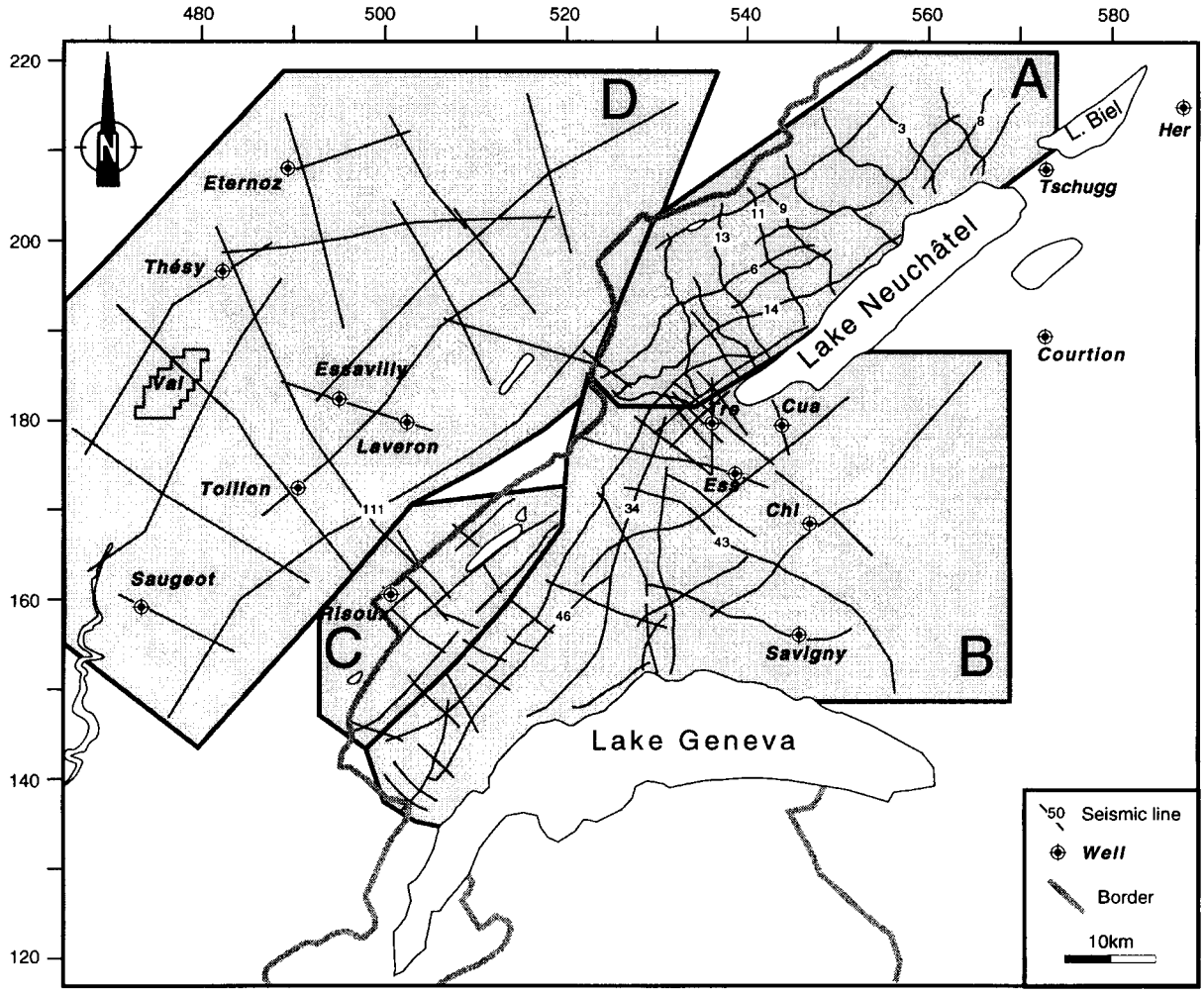

Fig. 5. Seismic data used in this work. Location of the various sectors: A = Neuchâtel and Vaud Jura. B = Molasse Basin. C = Mt-Risoux Jura. D = Champagnole-Mouthe Jura. Legend for drill holes: Chl = Chapelle; Cua = Cuarny; Ess = Essertines; Her = Hermrigen; Tre = Treycovagnes; Val = Valempoulières. Industry seismic reflection surveys were conducted in the study area between 1970 and 1988 by different companies: British Petroleum (sector A), Shell Switzerland (sectors B and C), Société anonyme des Hydrocarbures (sector B) and Shellrex (sector D).

2.2. The Molasse Basin

The clastic wedge of the Cenozoic Molasse Basin, presently considered a foreland basin (Price, 1973; Dickinson, 1974), is subdivided into three geological units, the Jura Molasse, the Plateau Molasse and the Subalpine Molasse (Homewood et al., 1989). The Jura Molasse represents the northern feather edge of the Molasse Basin that has been passively involved in Jura folding and thrusting. Only isolated patches of Molasse are preserved within major synclines of the internal Jura. The Plateau Molasse represents the major part of the Molasse Basin. The structures consist of broad anticlines oriented NE–SW and tear faults trending N–S, NW–SE and WNW–ESE. The northern limit of the Plateau Molasse corresponds to an erosional limit along the most internal, high amplitude folds of the Jura belt. The Subalpine Molasse is a narrow zone along the southern border of the Molasse Basin (Figs. 2 and 3). This zone is characterized by a stack of thrust sheets of Tertiary sediments, detached along a décollement zone located within these Cenozoic layers (Trümpy, 1980). The southern limit of this zone corresponds to the Oligocene Alpine front represented by the Alpine nappe stack (Prealps, Helvetic nappes, etc.) which overthrusts the Molasse sediments.

3. Stratigraphy

3.1. Regional overview

The Jura and the Molasse Basin consist of Mesozoic and Cenozoic sediments (Fig. 6) that are folded at variable degrees and which are detached from the pre-Triassic basement. The crystalline basement is nowhere exposed in the Jura and Molasse Basin. Basement in all of Swit-

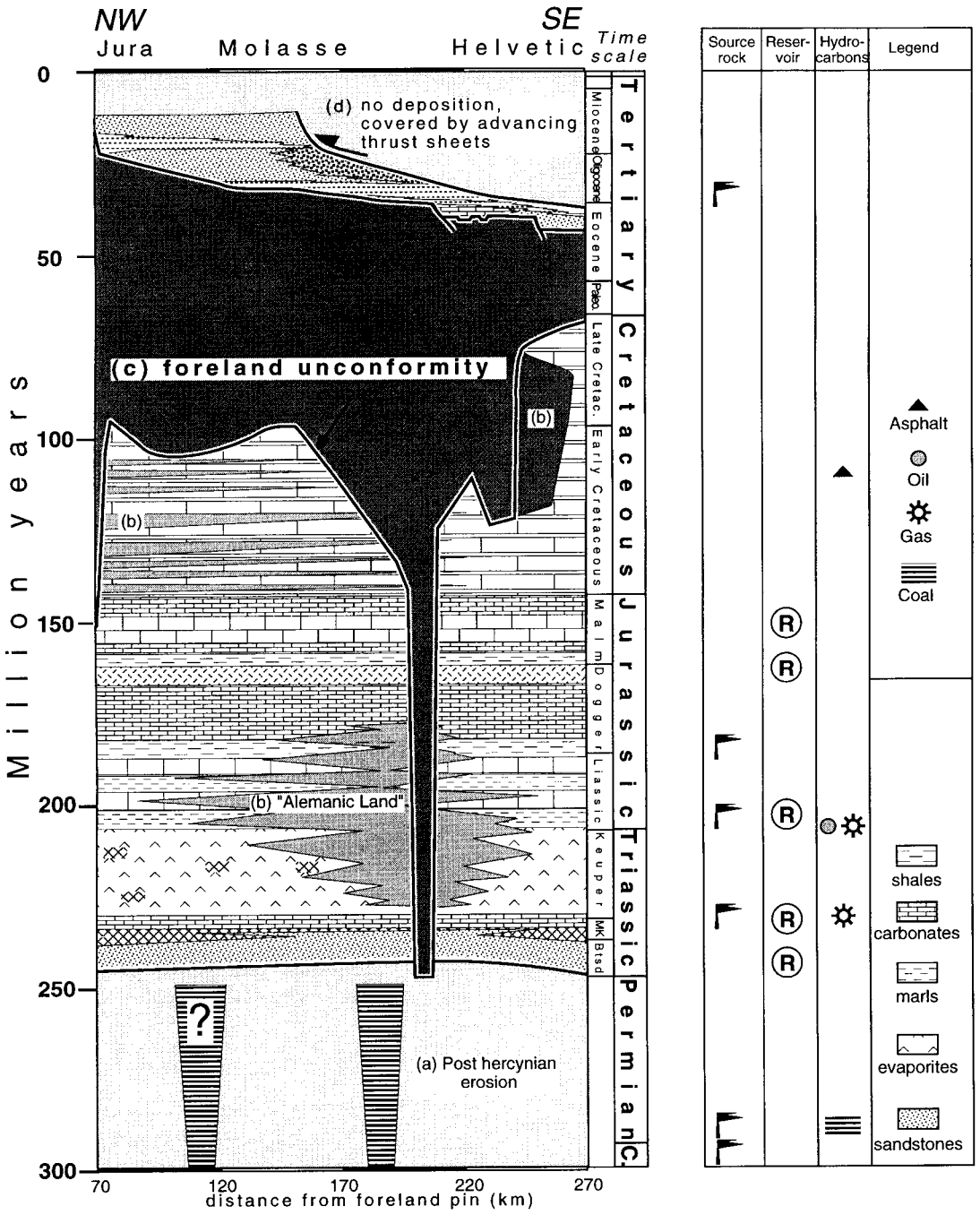

Fig. 6. Schematic stratigraphic/time section summarizing the most important Mesozoic and Cenozoic lithostratigraphic formations involved in tectonics of the NW Alpine foreland. The horizontal axis in km, measured from a pin in the foreland, is a restoration of the different paleogeographic domains. Vertical axis is time according to Palmer (1983). Major hiatuses are distinguished with different shades of gray, corresponding to (a) post-Hercynian peneplenation; (b) non-deposition or erosion during Mesozoic times including the so-called 'Alemanic land' and other important lacuna in the Cretaceous series on the craton side; (c) a pronounced foreland unconformity separating Mesozoic platform carbonate series from Tertiary foreland formations; and (d) Alpine collision and erosion. Oil occurrences are from Bitterli (1972) and Otto (1994). Figure modified from Burkhard and Sommaruga (1998).

zerland is composed of medium-to-high-grade metamorphic and plutonic rocks that were deformed during the Hercynian orogeny. The end of this orogeny is marked by the formation of narrow elongate grabens filled with Carboniferous and Permian lacustrine and fluvial series, including important Carboniferous coal measures and rare volcanic rocks. Coal seams result from burial of this organic matter (luxuriant continental vegetation). Although some of these E–W striking grabens are well known from drill holes (e.g., Lons-le-Saunier

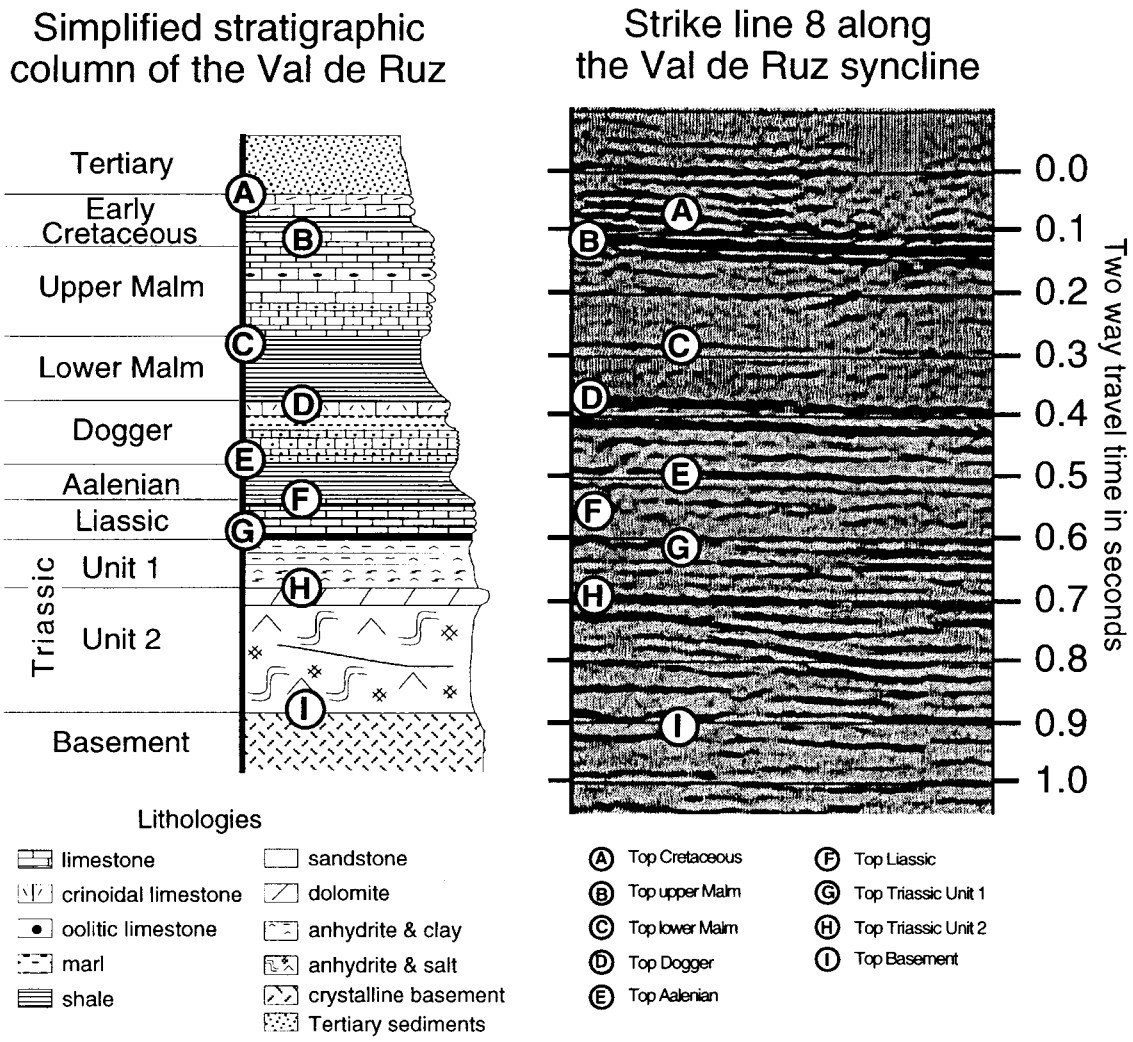

Fig. 7. Correlation of seismic reflectors (line 8, vertical scale in seconds, TWT) with simplified stratigraphic column of the Neuchâtel area. Letters A, B, C, ... represent the top of the seismic units used in this work.

basin located at the western edge of the Jura and the one located in the eastern Swiss Jura, Fig. 1) and from adjacent basement massifs, many more are still to be drilled below the Jura and Molasse where they were poorly imaged at present (Fig. 8). The basement is therefore characterized by two major unconformities: one below the Carboniferous sediments and a second below the Triassic rocks.

The Alpine cycle sensu lato started with peneplanation and a subsequent transgression in the Early Triassic and after the Jurassic time, the Jura and Molasse Basin realm became part of the Alpine Tethys passive margin. During the Triassic, up to 1 km of evaporites and shales accumulated in an elliptical depo-center in the area of the future Jura arc (Fig. 9). Limestones of Dogger and Malm age form the backbone of folds and crop out in the eastern and central Jura, whereas Lower Cretaceous limestones form the crests of the western Jura anticlines. During the Oligocene and Miocene, fluvial, lacustrine and marine clastic Molasse sediments were deposited in the Alpine foredeep. They progressively onlap the underlying Mesozoic rocks toward the northwest. This basal Tertiary unconformity (Fig. 6) is the only obvious unconformity on our seismic lines. The thickness of this Tertiary wedge decreases from south (up to 4 km) to north (a few hundred meters). These series crop out mainly within the Molasse Basin but are also partially preserved in the Jura synclines. For more details on the evolution of the northwestern foreland, see discussions in Ziegler et al. (1996) and Burkhard and Sommaruga (1998).

Thanks to the good quality of the seismic lines, it has been possible to constrain the deep stratigraphy, which is especially important for Triassic layers that are not exposed in the studied area. The total thickness of the Mesozoic layers below the Neuchâtel Jura from top Cretaceous to the base of Triassic Unit 2 appears to be about 2000 m with an estimated uncertainty of about ± 200 m. Jurassic layers thicken progressively from Neuchâtel

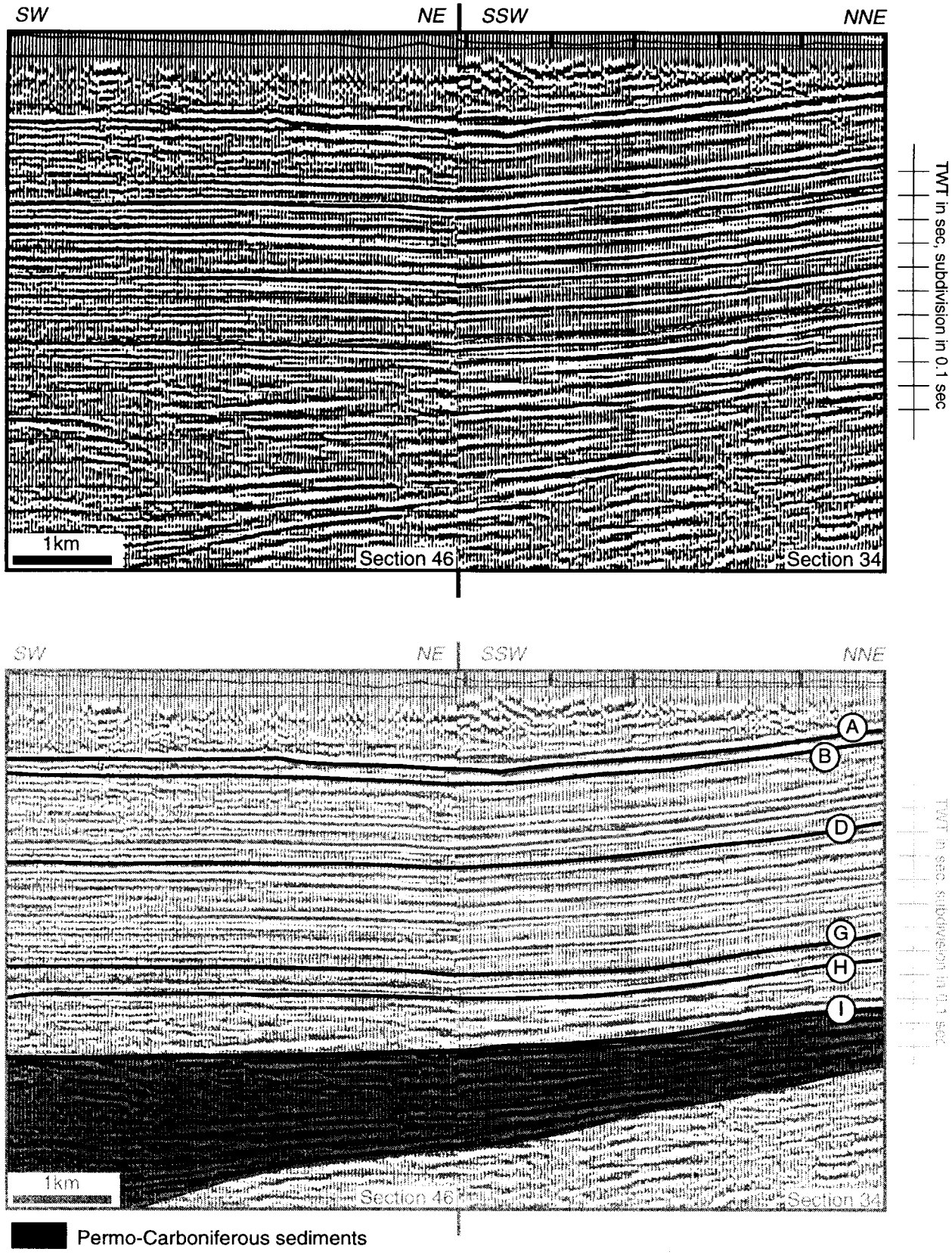

Fig. 8. Seismic section showing Permo-Carboniferous sediments under the Mesozoic cover. Legend for the top of the layers: A = Lower Cretaceous or base Tertiary; B = upper Malm; D = Dogger; G = Triassic Unit 1; H = Triassic Unit 2; I = Basement. For location, see map in Fig. 13.

towards the southwest (Geneva) and decrease slightly toward the northwest (Besançon).

3.2. *Oil occurrences*

According to Bitterli (1972), Otto (1994) and Ziegler et al. (1996), major source rocks in the Jura belt and the western Molasse Basin are (Fig. 6): Stephanian and Early Permian lacustrine series including meter-thick coal measures contained in wrench-induced grabens; Triassic and Liassic organic shales (Lettenkohle, Posidonia- and Opalinum- shale), which are mature for oil generation under the Molasse Basin; Early Oligocene Flysch (Meletta shale). The latter is restricted to the internal border (S–SE) of the Molasse Basin. All these series reached the oil- or gas window (at the Alpine front) during Middle to Late Miocene in response to burial by the Molasse wedge. Little is known about the precise relative timing of hydrocarbon generation, migration and deformation of the Molasse Basin and Jura fold-and-thrust belt. However, the asphalt deposits from the Neuchâtel Jura (Meia, 1987) of which the source beds are still unknown, indicate that the asphalt must have migrated before the deformation of the Jura (Zweidler, 1985).

Proven reservoirs occur within the Lower Triassic Buntsandstein and Middle Triassic carbonate series sealed by Upper Triassic evaporites and shales. Jurassic reservoir rocks include Malm reefs, and various oolite-series (Malm and Dogger ages). In the Haute Chaîne Jura, however, the latter have negligible cover and insufficient seals which may explain the widespread occurrence of seeps and asphalt deposits along the Jura/Molasse Basin border. Potential, non-explored reservoirs are related to sub-salt Triassic series, charged by Permo-Carboniferous source rocks and to Mesozoic carbonates and sands, charged by Early Jurassic sources rocks and sealed by basal Oligocene marine shales (Ziegler et al., 1996).

3.3. *Seismic units*

Seismic units correlated in this work do not represent sequences as defined by Mitchum and Vail (1977). Our seismic data are not sufficiently differentiated to allow for sequence stratigraphic interpretation. As used here, a seismic unit is sandwiched between two strong continuous reflectors, corresponding to major impedance (lithologic) changes, i.e., marl/limestone or shale/limestone (labeled from A to I, Fig. 7). Based also on wells, seismic stratigraphic units have been identified and correlated through the whole seismic grid jumping from one limit to another. Strike profiles, mainly shot in synclines, are good to excellent and show subparallel reflectors that are most useful for the stratigraphic interpretation (e.g., Fig. 15). Dip profiles are less continuous, owing to steep to vertical dips, complicated structures and rugged topography (e.g., Fig. 14). This research highlights especially the Triassic Units, because they are a key to understand the Jura fold belt development. The Triassic Unit 1, as defined on seismic lines, has a fairly constant thickness around 200 m, whereas the Triassic Unit 2 interval varies in thickness and commonly has oblique reflectors on the seismic lines (e.g., Fig. 7). These oblique reflectors could be interpreted as tectonic structures (see discussion on structure examples) just above the main décollement horizon. Thickness changes within the Triassic Unit 2 are presented on an isopach map (Fig. 10), which correspond to the depth-converted interval from reflector H to I. The thickness varies considerably and ranges from 300–1200 m. In addition to a general trend of thickening towards the NW, the isopach map shows a conspicuous series of lows and highs, on a 10-km wavelength with a strong NE–SW trend, parallel to the Jura folds further to the north. The highs are interpreted in terms of stacks of evaporites, clays and salt, that developed during the deformation of the Jura and Molasse Basin. In contrast, the thickness of Triassic Unit 1 ranges from 400–200 m, decreasing progressively toward the ESE.

During the Triassic, more than 1000 m of sediments accumulated in the area of the future Jura arc. In contrast some 60 km further south in the North Helvetic domain (Fig. 6), less than 50 m of sediments were deposited in the same time span. Despite this considerable lateral variation, no evidence for synsedimentary faults has been detected. Important lateral thickness variations in the Triassic on the scale of about 10 km are related to Miocene deformation and material redistribution within this weak layer, which served as the major décollement horizon for Jura tectonics.

4. Structures

On a large scale the Jura arc shows all characteristic features of a foreland fold-and-thrust belt that developed above a weak basal décollement (Davis & Engelder, 1985; Rodgers, 1990; Laubscher, 1992). These features include the arcuate outward convex shape, folds, thrusts and tear faults, that are all kinematically compatible with a tectonic transport in a general NW direction. Surface observations, and especially seismic subsurface data, display two different types of folds: evaporite-related folds and thrust-related folds. The Molasse Basin and the external Plateau Jura present broad, long-wavelength, low-amplitude folds cored by Triassic evaporites; by contrast, the Haute Chaîne Jura is characterized by high-amplitude folds which formed above thrust faults stepping up from the basal Triassic décollement zone.

4.1. *Evaporite-related folds*

Low-amplitude folds may be difficult to recognize on geological maps or in the field. The low limb dip and

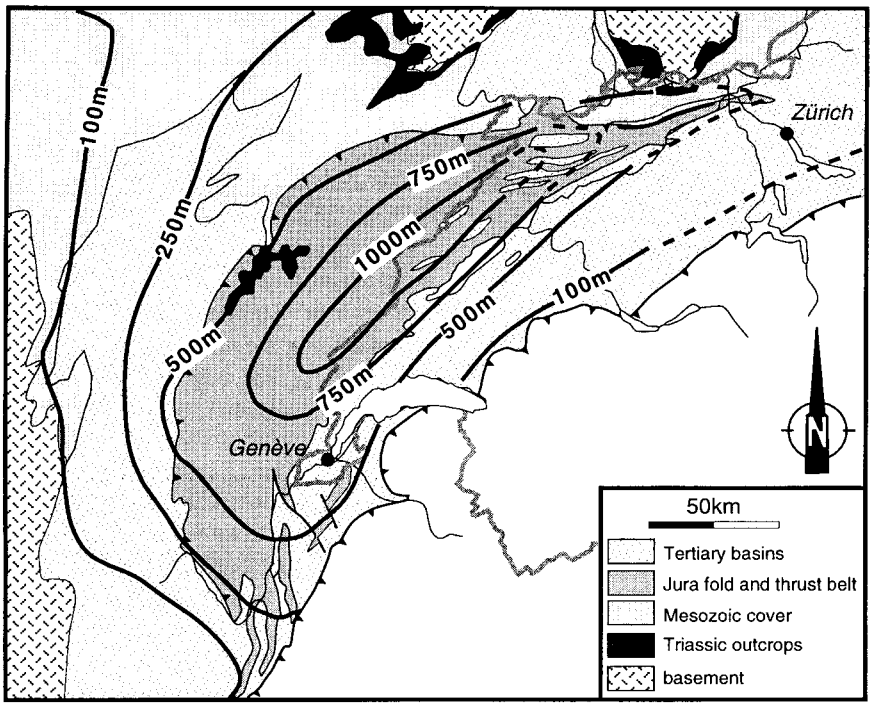

Fig. 9. Isopachs (in meters) of the Triassic layers (minus Buntsandstein) in the Jura fold-and-thrust belt and adjoining areas. Thicknesses are compiled from several authors (Bachmann et al., 1987; Bitterli, 1992; Debrand-Passard & Courbouleix, 1984; Winnock et al., 1967)

relief make these structures inconspicuous. Seismic lines are more useful in documenting the geometry of this fold type at depth. Interpretations of seismic lines across the Plateau Jura and the Molasse Basin, show a series of broad and gentle anticlines that are controlled by evaporite, salt and clay stacks within the ductile Unit 2 of the Triassic layers. In the scientific literature, this type of anticline is termed salt anticline or salt welt (Harrison & Bally, 1988). In this work, we prefer to use the terms evaporite cored anticline, due to the uncertainty about the amount of pure salt in the Triassic layers. Conventional diapirs, as first visualized by Trusheim (1960), are today often interpreted as being of extensional origin (Vendeville & Jackson, 1992a; 1992b; Jackson & Vendeville, 1994). Salt pillows are contractional buckles (Coward & Stewart, 1995); the evaporites pinch out in the adjacent synclines and flow into anticlinal evaporite ridges (Harrison, 1995), as is the case for the Jura.

The Plateau Jura broad fold type is illustrated on the Section 111 in Fig. 11. This fold displays two long asymmetric limbs dipping with a very low angle towards the north and the south respectively. This geometry is illustrated by a well-layered series of reflectors in the middle of the Mesozoic cover series. This apparently tectonically undisturbed sequence represents the evaporites of Triassic Unit 1. Beneath this unit are discontinuous reflectors of Triassic Unit 2. Some of these reflectors onlap the deepest strong and continuous reflection, which represents the top of the basement (which may be either crystalline rocks or Permo-Carboniferous sediments). The Triassic Unit 2, highlighted in dark gray on Fig. 11, increases in thickness from NW to SE probably owing to evaporite stacking. It is the thickest stack of evaporites ever observed in the central Jura and has moreover been confirmed by the Laveron drill hole (BRGM, 1964).

In the Molasse Basin, broad anticlines are known from outcrop geology. Interpreted subsurface data present a succession of low-amplitude folds, with gently dipping limbs (Fig. 12). Folds with a high degree of symmetry have been found in the southern region, whereas farther to the north they are either foreland- (NW) or hinterland- (SE) verging. The same anticline may also change its vergence along strike. The geometry of the folds is highlighted by a well-layered series of reflectors representing Cretaceous, Jurassic and Upper Triassic strata. The core of these folds is filled with thickened Triassic Unit 2 beds; their geometry is shown in detail on seismic examples of Fig. 12 (for location of these parts of seismic lines see Fig. 10). The Triassic isopach map highlights elongated or elliptical thickening of the Triassic Unit 2 along a NE–SW trend. The maximum thickening underneath broad anticlines coincides with the most internal Jura anticlines. Generally, Unit 2 displays discontinuous reflectors, which are either flat or oblique, bounded by a basal and a roof reflector. Figure 12 shows a succession of oblique reflectors within Triassic Unit 2, which may be inter-

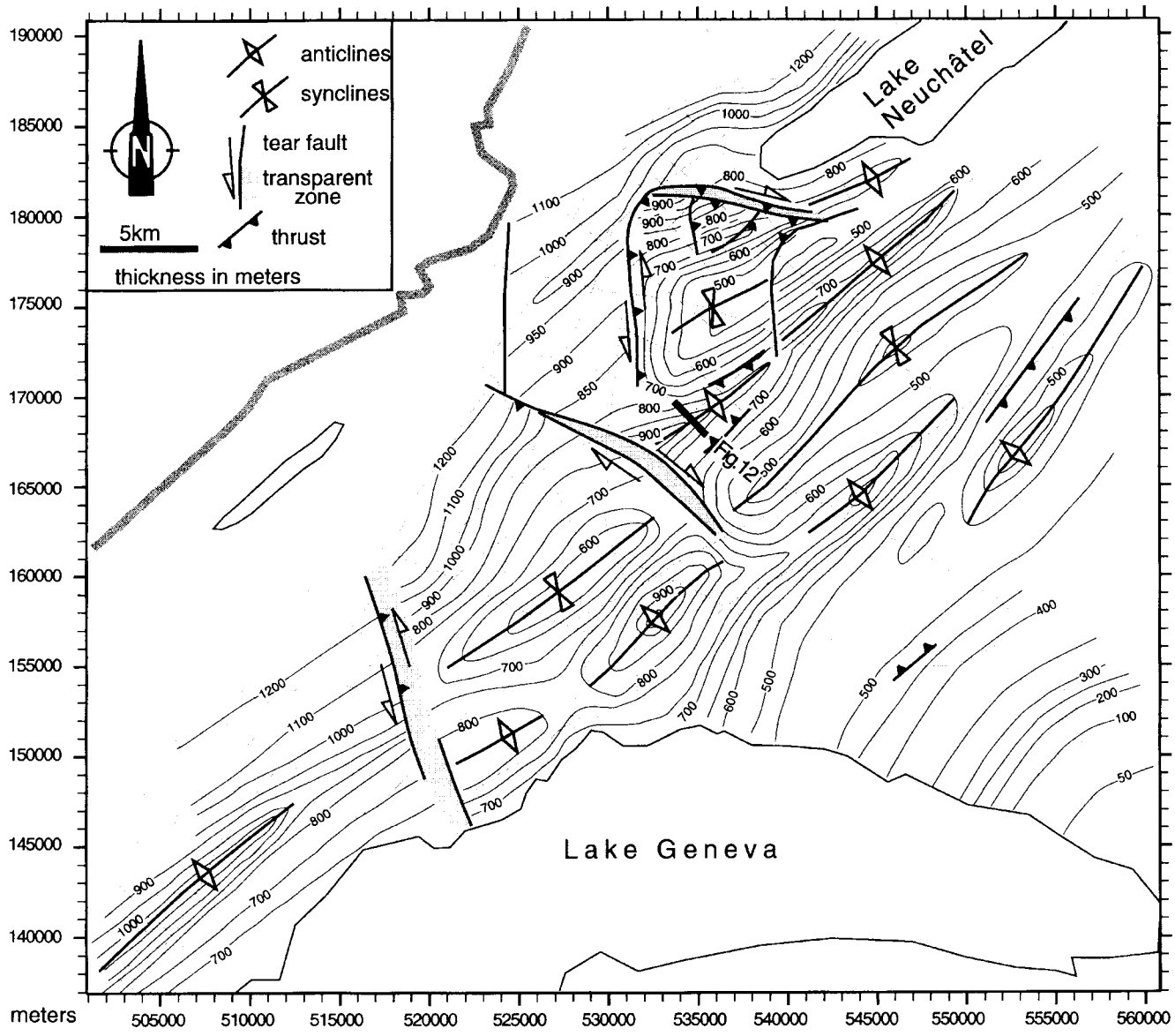

Fig. 10. Isopach map of the Triassic Unit 2 beds from the western Molasse Basin. Anticline axial traces emphasize thick zones, syncline axial traces show thin zones. Coordinates in meters are according to the Swiss geographic reference grid. Modified from Sommaruga (1995).

preted as small thrust faults imbricating parts of the unit (Mitra, 1986; McClay, 1992, duplexes) resulting in its overall thickening. According to the classification of Boyer & Elliott (1982), these structures may correspond to hinterland dipping duplexes within an anticlinal core. Development of such structures, that confined to the lower unit just above the basement, caused folding of the mainly unfaulted overlying layers. The roof thrust of the duplex is just below reflector H.

True salt flow producing the so-called evaporite anticlines is not proven in the Jura fold-and-thrust belt, nor in the Molasse Basin. The Laveron well log, which shows more than 300 m of cumulative thickness of several beds of pure salt of the Triassic Units, is the thickest pillow (1400 m thick) observed in the studied area (Fig. 11). On the seismic line, the reflectors do not highlight any structural relationship; they may represent changes of lithology. The thick salt and the absence of structural features suggest that the thickening within the Triassic Unit 2 is indeed the result of an accumulation of salt and evaporite by lateral flow. This flow occurs in a compressional regime and is not to be confused with conventional salt diapirism, which often occurs in an extensional context. Moreover, these fold cores are not diapirs, because they have concordant contacts. It is important to underline, that no salt diapir occurs in the

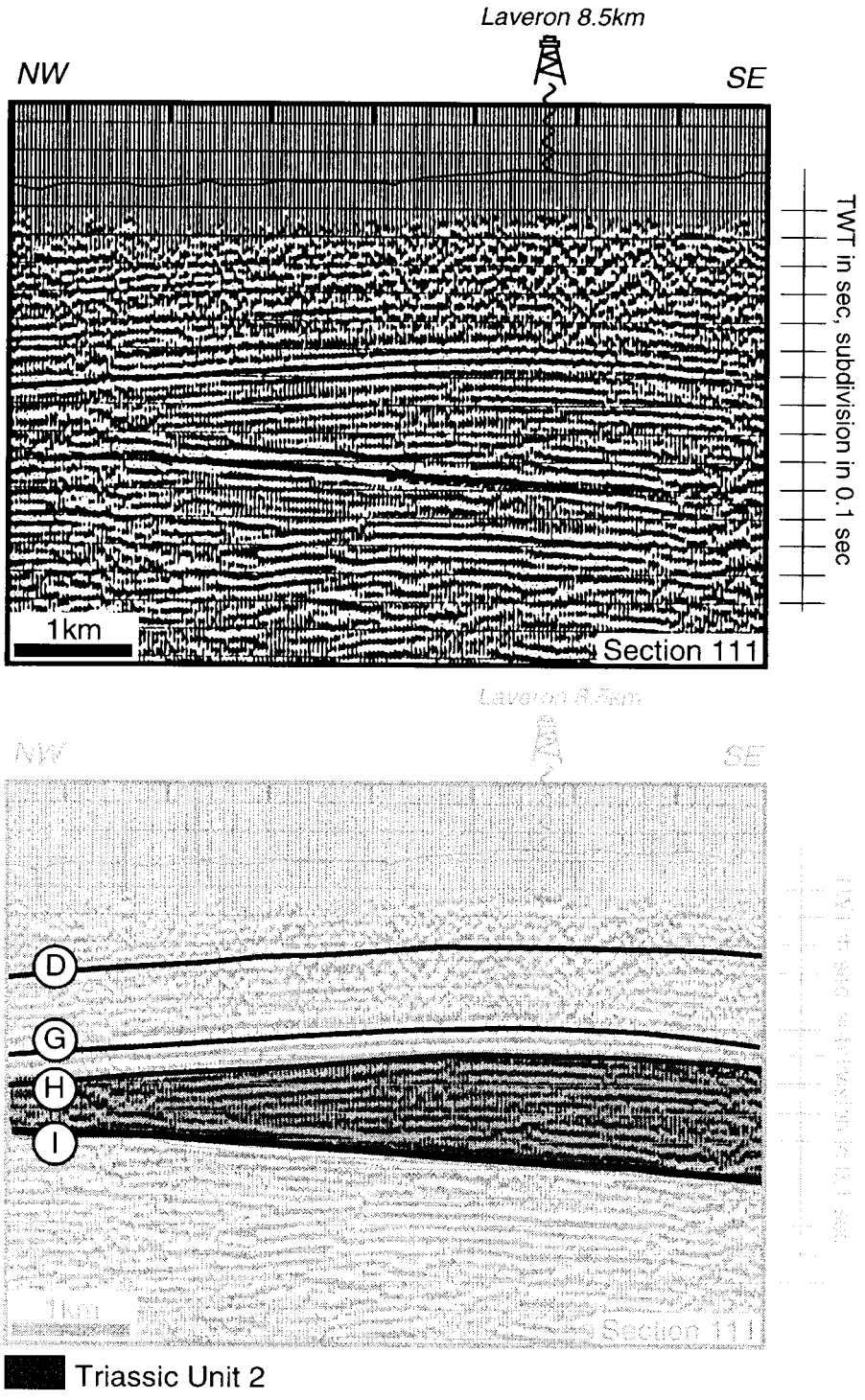

Fig. 11. Evaporite-related anticline on the dip seismic Section 111 located in the Plateau Jura (external zone). The interpretation displays a broad anticline related to thickening of the Triassic Unit 2. Laveron drill hole (projection), which reaches the top of the Early Triassic strata, confirms the seismic interpretation. Legend for the top of the layers: D = Dogger; G = Triassic Unit 1, H = Triassic Unit 2. For location, see Fig. 13.

Jura belt and the Molasse Basin. This is probably because of the scarcity and thinness of pure rock salt layers in the Triassic series and the lack of early extension or differential sedimentary loading.

4.2. Thrust-related folds

The classic sinusoidal shape of the Jura folds as drawn by earlier geologists (Heim, 1921; De Margerie, 1922)

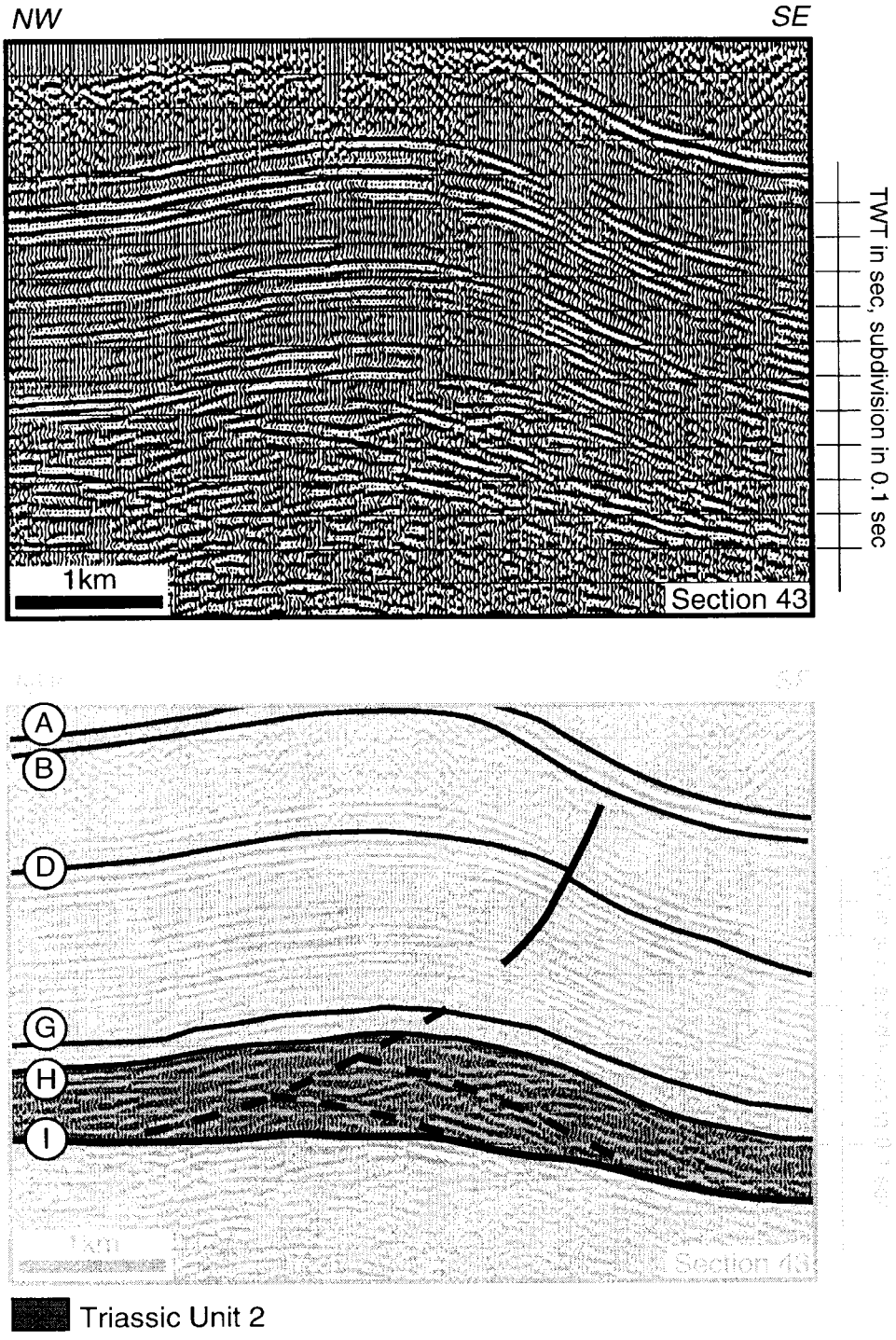

Fig. 12. Evaporite-related anticline on the dip seismic Section 43 from the western Swiss Molasse Basin. For location, see Figs. 10 and 13. The interpretation shows a hinterland-vergent fold related to thickening within the Triassic Unit 2. The thickening may be due to duplex structures. Legend for the top of the layers: A = Lower Cretaceous or base Tertiary; B = upper Malm; D = Dogger; G = Triassic Unit 1, H = Triassic Unit 2.

has been shown to be an oversimplification, not only in the central, but also in the eastern (Laubscher, 1977) and western Jura (Philippe, 1994). In most places, at the surface, a veneer of Quaternary sediments obscures the critical relationships between strata and thrust faults. Seismic data have, however, confirmed that some folds are related to major thrust faults (Figs. 14 and 16).

On many profiles, velocity anomalies correspond to a small positive deflection of the reflectors beneath anticlines (velocity pull-up) and a negative deflection beneath synclines (velocity pull-down). The dip Section 3 (Fig. 14) and the strike Section 8 (Fig. 15) from the Neuchâtel

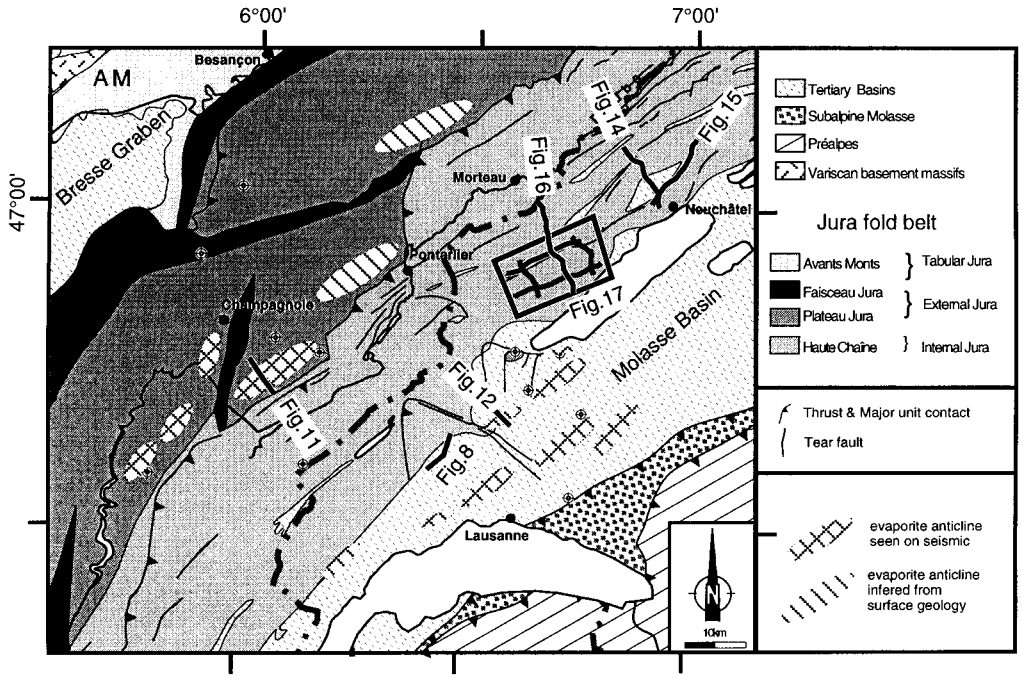

Fig. 13. Tectonic sketch of the Jura and Molasse Basin with the disposition of the evaporite-related anticlines interpreted on seismic or inferred from surface geology. Figure numbers show location of the seismic lines presented in this paper.

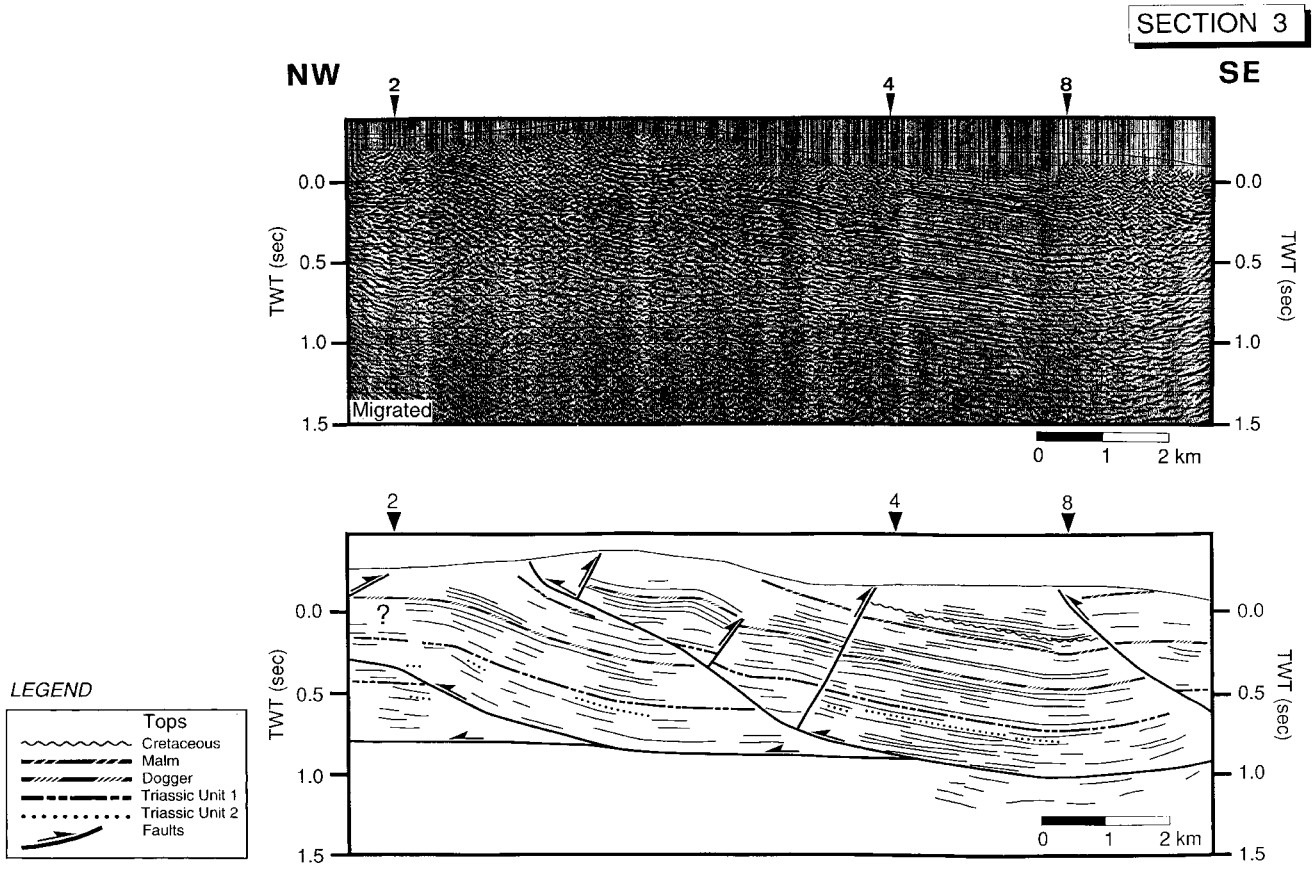

Fig. 14. Section 3: uninterpreted migrated dip seismic section and line drawing, showing a thrust-related anticline, located in the Neuchâtel Jura (Switzerland). La Ferrière-Vue des Alpes tear fault, located at the northern end of the major anticline is not recognizable on the seismic line. For location, see map in Fig. 13.

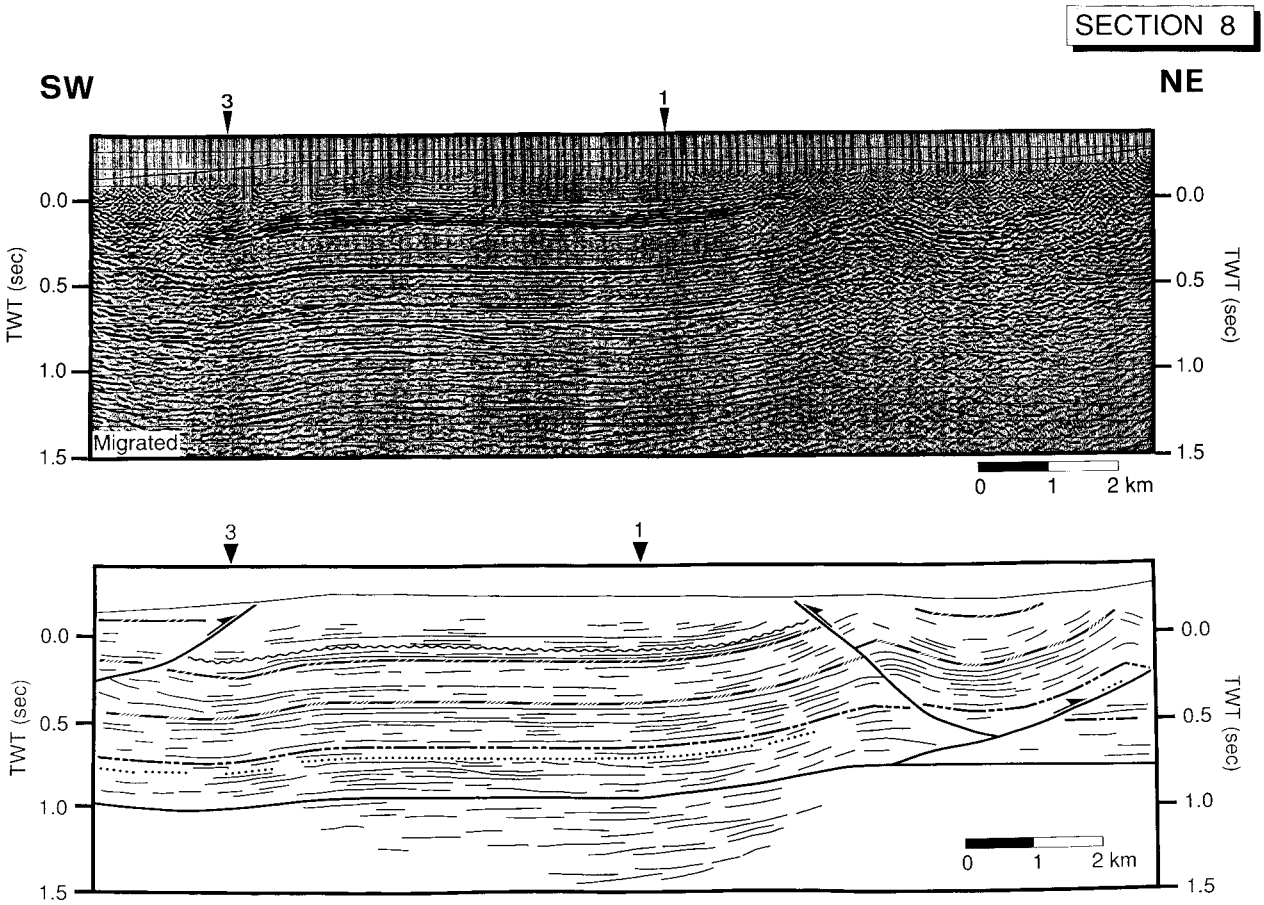

Fig. 15. Section 8: uninterpreted migrated strike seismic section and line drawing, located in the Neuchâtel Jura (Switzerland). For location, see Fig. 13.

Jura illustrate such anomalies, which disappear on the depth conversion of these lines. Transverse lines crossing the Jura, oriented perpendicularly to the fold axes (NW–SE), allowed the fold geometry to be constrained at depth. These high-amplitude folds, which are asymmetric and are related to thrust faults, root in the basal décollement zone within the evaporites of the Triassic Unit 2. These thrust-related anticlines duplicate the entire Jurassic sequence (Figs. 16 and 17). One such duplication in the Mt-Risoux anticline (Vaud area) has been confirmed by drill hole (Winnock, 1961). Thrust-related anticlines are separated by broad or tight synclines. Many thrust faults are NW (NNW)-verging (Figs. 14, 16 and 17), like the main thrust system (foreland-vergent thrust). SE (SSE)-vergent thrust faults are considered as backthrusts (hinterland-vergent thrusts). Foreland-vergent thrusts have at least kilometric dip slip (e.g., Section 11, Fig. 16 or 17) and hinterland-vergent thrusts generally have few tens or hundreds or meters of displacements. Thrust faults include both flats and ramps. All mapped foreland-vergent thrust faults reach the surface, breaking through the structures in the steep frontal limbs. Anticlines and synclines in the Risoux Jura have a lateral continuity over 30 km, whereas in the Neuchâtel Jura the lateral continuity is limited to 10 km.

The foreland-vergent thrust ramps dip between 20–30 or more, whereas backthrusts in the Neuchâtel Jura are much steeper (±60°). These angles are approximate, because they are deduced from the seismic time profiles.

Rheological contrasts within the sedimentary multilayer cover are responsible for the fold-and-thrust geometries. A high strength contrast also exists between the very weak Triassic Unit 2 layer and the weak to strong overlying layers. The Haute Chaîne Jura folds were initiated first as buckle folds in response to the layer-parallel compression (Fig. 18). These embryonic detachment folds, subsequently developed into fault-propagation folds and fault-bend folds after breakthrough of thrusts, with further deformation. According to Dixon and Liu (1992), a similar evolution of folds has been observed in centrifugal structural models, subjected to horizontal, layer-parallel compression.

4.2. Tear faults

Some seismic lines cross major tear faults, e.g., the Pontarlier fault (Fig. 19). These faults are defined here as

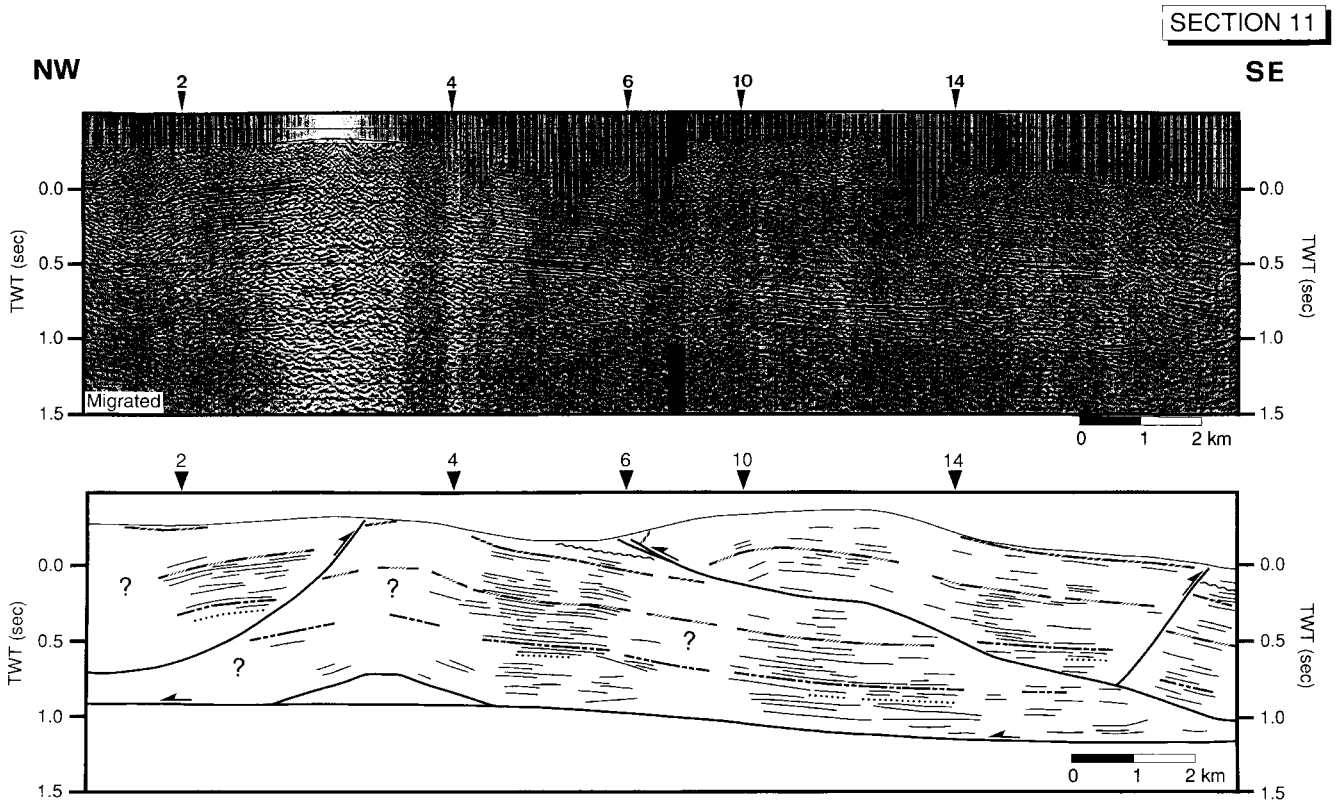

Fig. 16. Section 11: uninterpreted migrated dip seismic section and line drawing, located in the Neuchâtel and Vaud Jura (Switzerland). This line presents a thrust-related anticline with duplication of the Mesozoic series. For location, see Fig. 13.

belonging to an allochthonous cover with a transcurrent movement and terminating into a décollement zone (Dahlstrom, 1970; Twiss & Moores, 1992). These faults appear on seismic lines as transparent zone. They affect the whole Cenzoic and Mesozoic cover but do not show any offset of the basement top within the seismic resolution. In the Neuchâtel area, seismic data along tear fault zones of La Tourne and La Ferrière-Vue Alpes (Section 3, Fig. 14) are of poor quality, probably owing to the presence of an anticline on one side of the faults. Therefore, these faults are not recognizable on seismic lines. However, seismic data crossing the southern part of the major Pontarlier tear fault are of high quality on both sides of the fault. The tear fault appears to terminate in the décollement zone of Triassic Unit 2. Accordingly these previous mappable faults are either tear faults restricted to the cover or related to lateral ramps. No evidence for an extension of these faults into the basement could be found (compare Figs. 10 and 20), though this possibility cannot be eliminated with the low resolution of the seismic data at depth.

Tear faults in the Jura are well known from geological maps (Fig. 2) but can almost as well be recognized on topographic maps, whether traces appear to be straight lines or narrow linear depressions even across rugged topography. In this respect, seismic lines and cross-sections, do not contribute much to the analysis of strike-slip tectonics. Strike-slip faults sensu lato are best analyzed on the horizontal plane of geological or geomorphological maps or time slices, which are natural sections that contain the dominant displacement vector. In the Jura, a close genetic relationship between folding and tear faults was postulated by Heim (1915), who noted the radial arrangement of the tear faults on a map of the entire Jura arc (Fig. 19). Major, apparently sinistral, tear faults are oriented NW–SE in the southern Jura, NNW–SSE to N–S in the central Jura and NNE–SSW in the eastern Jura. Somewhat shorter, apparently conjugate dextral tear faults are less common. Folds, thrusts, sinistral and dextral tear faults define a set of structures compatible with a horizontal shortening in a WNW–ESE, NW–SE, and NNW–SSE direction respectively (Laubscher, 1972, indenter model).

5. Discussion and conclusions

Depth conversion of all seismic lines has allowed mapping of the depth to top basement in the central Jura and the Molasse Basin (Fig. 20). In the Jura area, a simple velocity model, attributing a constant velocity to each major seismic unit has been used. In the Molasse Basin,

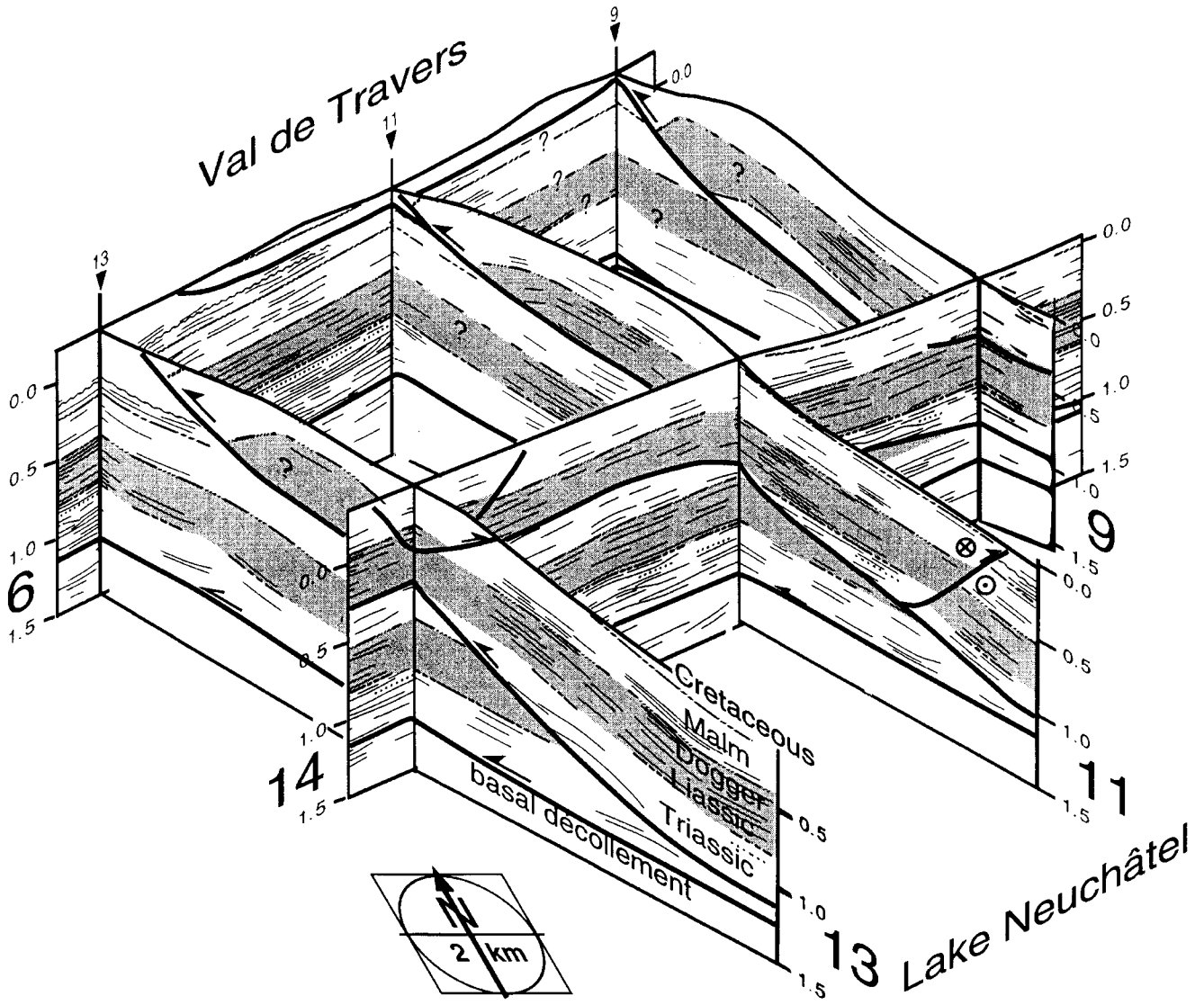

Fig. 17. Fence diagram of dip and strike seismic lines from the Neuchâtel and Vaud Jura, Switzerland. This figure presents the lateral continuity of a thrust-related anticline. For location, see map in Fig. 13. Modified from Burkhard et al. (1998).

however, more complex depth-dependent conversion functions from Naef and Diebold (1990) were used in order to account for increased velocities due to the considerable thickening and facies changes of Tertiary sediments. The contour map highlights a rather smooth basement that dips uniformly at 1–3 to the SSE. Depths from well data (e.g., Treycovagnes, Laveron, Essavilly, Valempoulières) fit to ±200 m, the depths obtained from depth converted seismic time lines. Discrepancies may be due to the use of inappropriate seismic velocities, especially in the weathering layer (Schnegg & Sommaruga, 1995). However, seismic velocities used in this work are compatible with the overall well information but do not precisely match individual drill hole data. The trend of the basement is E–W in the Neuchâtel Jura and NE–SW or ENE–WSW in the other regions (Risoux, external Jura and Molasse Bain). The E–W trend of the Neuchâtel Jura differs by an angle of 30 from the orientation of structures in the Jura fold-and-thrust belt. The major tear faults (e.g., Pontarlier, La Sarraz) do not show any significant offset of the basement top. Along these faults, data are reasonably well constrained in the Molasse Basin and no major bend is visible. The tear faults are therefore limited to the sedimentary cover of the Jura. In addition, evaporite-related folds and thrust-related folds are floored by subhorizontal layers at their base. Nowhere in the study area has this basal décollement layer been disrupted by later thrusts. Any irregularities which exist in the top of the basement are probably small compared with the thickness of Triassic Unit 2, which ranges from 100 m to more than 1000 m. On the southeastern edge of the map (Fig. 20), near the front of the Subalpine

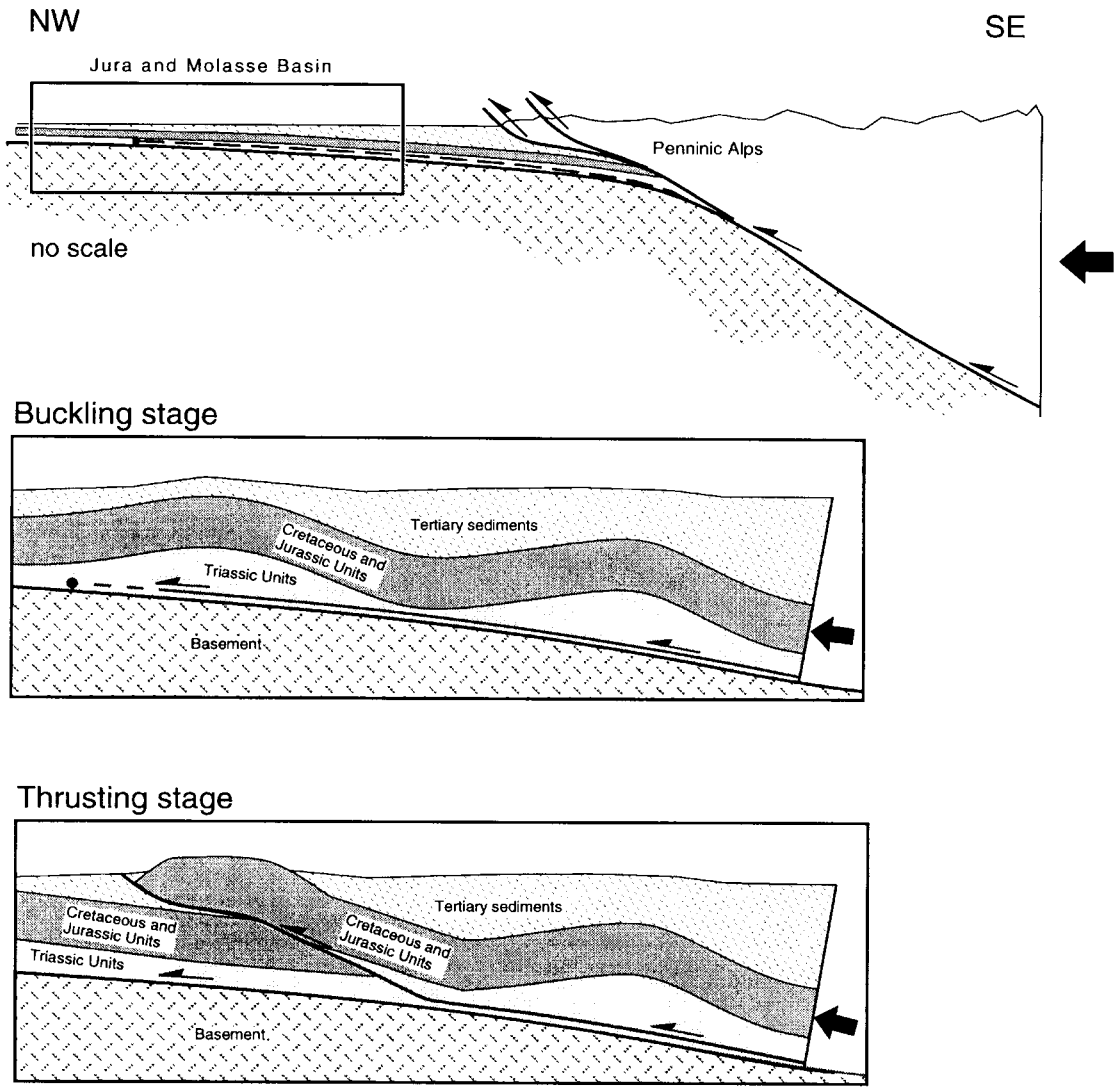

Fig. 18. Conceptual evolutionary stages of the Jura foreland between 20–15 Ma. This sketch is without scale.

Molasse, the basement dips locally toward the north, showing an important uplift. This basement high results either from an inversion of a Permo-Carboniferous graben (Gorin et al., 1993) or else a basement slice. No reflector appears beneath the supposed basement top, so it is difficult to interpret the nature of this high.

In the Molasse Basin, the basement top map (Fig. 20) contrasts significantly with the isopach map of Triassic Unit 2 (Fig. 10). The changes in thickness along a NE–SW trend suggest 'ductile' deformation within Triassic Unit 2. The isopach map of both Triassic Units (Fig. 9) in the Jura and its vicinity has been compiled in order to examine possible correlation between the distribution of Triassic strata and the extent of the deformed Jura cover. A rather good correlation between both may be inferred from Fig. 9. The thickest regions correspond to the central Haute Chaîne Jura and to the southern part of the external Jura. Towards the southwest, several drill holes have demonstrated the absence of evaporitic layers (Philippe, 1994; Philippe et al., 1996); Triassic salt pinches out toward the future Aar massif (Ziegler, 1990). It therefore appears likely that the existence, as well as the arcuate shape of the Jura fold-and-thrust belt, is intimately linked to the presence of Triassic evaporites (Letouzey et al., 1995).

As described above, the central Jura and the Molasse Basin display two different types of folds: thrust-related folds and evaporite-related folds. The first type is located in the Haute Chaîne Jura, whereas the second type is present in the Plateau Jura at the very front to the northeast of the Haute Chaîne Jura folds, and beneath the Molasse Bain. These two types of folds are respectively interpreted as evolved and embryonic stages of the late Miocene cover deformation (Sommaruga, 1997). Folds are thought to evolve from low-amplitude, apparently symmetric, buckle folds in response to layer-parallel com-

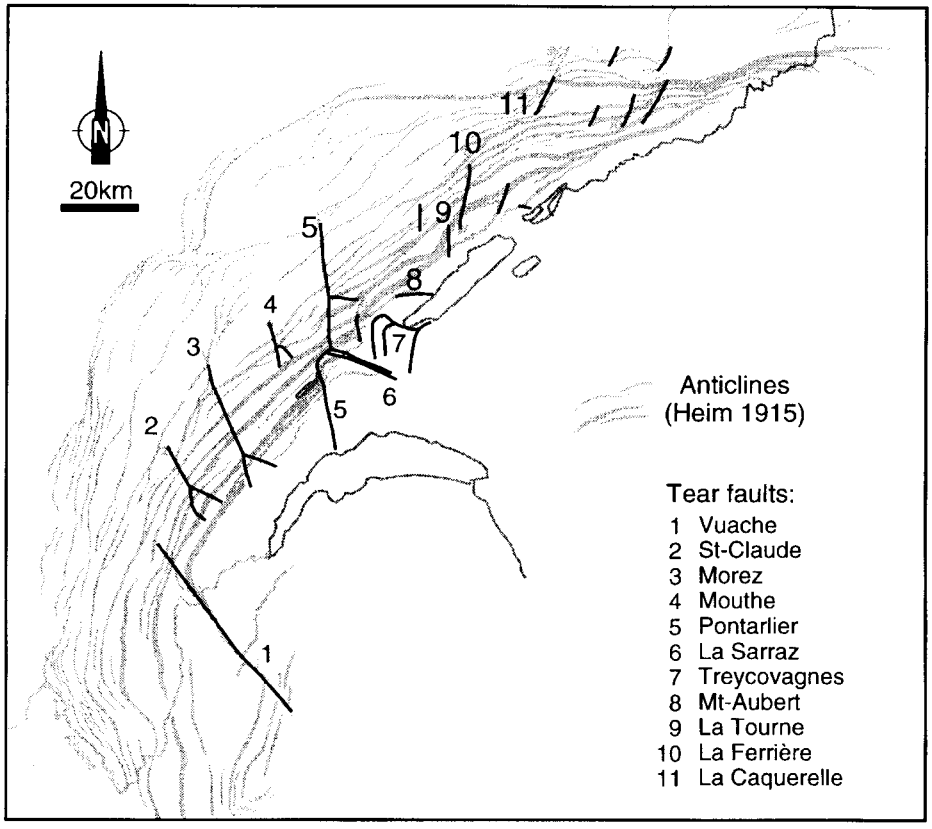

Fig. 19. Location of tear faults on the Jura anticline map drawn by Heim (1915).

pression (Fig. 18). The very weak evaporite rocks of the Triassic series infilled the space generated at the base of the sedimentary cover by rising anticlines. The very weak basal zone thickened in the core of the anticlines, whereas the strong layers buckled with no change of thickness (parallel folding). With further deformation, fault ramps nucleate in the hinge area at the base of the strong layers in order to accommodate further shortening. Fault ramps then propagate upward within the stiff layers or bend within overlying weak or incompetent layers. With further transport, the cover may be doubled, as observed in the present day Haute Chaîne Jura folds. The spacing between adjacent early-stage buckle folds should be large, since in the Haute Chaîne Jura the formation of subsequent folds does not alter the geometry of the adjacent folds. This tentative explanation of the evolution of thrust-related folds is based on the observation of various evolutionary stages across the western Jura fold thrust belt. Low-amplitude anticlines related to salt welts are also well illustrated by Harrison and Bally (1988) and Harrison (1995) on high-quality seismic data from the Parry Islands Fold Belt (Melville Island, Canadian Arctic). The increasing intensity of deformation toward the hinterland can be viewed as representing evolutionary stages of deformation and, as a result, gives insight into the evolution of deformation within large anticlines. In Melville Island, thrust faults appear to be progressively younger from bottom to top. In comparison, the Jura Plateau and the Molasse Basin folds seem to be less evolved, since no obvious 'fishtail' wedging is observed above the salt welts.

Along strike in the Jura belt, we observe fold style variations: imbricated thrust sheets in the southwestern area (Philippe et al., 1996), large thrust-related anticlines in the central part (Laubscher, 1965; Sommaruga, 1997) and symmetric folds, lift-off-fold or box-fold type in the northeastern area (Buxtorf, 1916). These changes in deformation styles (Philippe et al., 1996) are related to the nature and rheology of the décollement zone (pinch out of the Keuper salt to the southeast), to the amount of bulk shortening, to a northeastward decrease in the thickness of the stiff Late Jurassic layer and a concomitant increase of both number and relative proportion of incompetent layers, Triassic and Aalenian layers.

According to Bally et al. (1966) and critical taper models (Dahlen et al., 1984), orogenic fold-and-thrust belts evolve by progressive deformation from the hinterland to the foreland. If we admit this consideration as a rule, the southernmost structures of the Jura fold-and-thrust belt should have formed first, then evolved into the present day structures. The northern folds should therefore represent a later stage of deformation, with less evolved geometries. The folds beneath the Molasse basin are located into a more internal position of the Alpine fore-

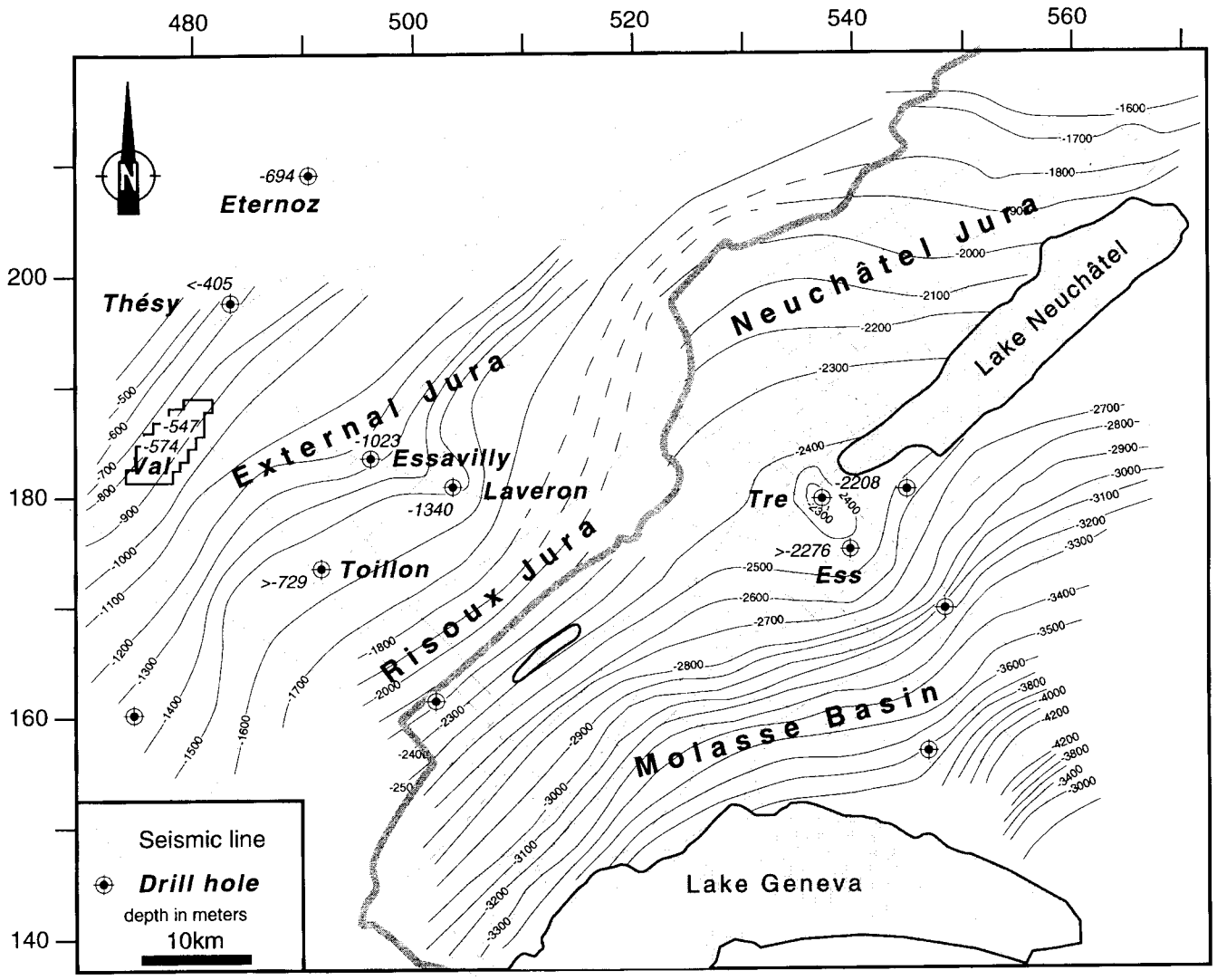

Fig. 20. Map of the depth to top basement in the central Jura and western Molasse Basin. Depths are in meters with reference to the sea level. Depths next to drill holes correspond to top basement depth from drill hole data. Minimal depths (>...) are given from drill holes which ended within the Triassic layers. No depth indication is given for drill holes that did not reach the Triassic. Legend for drill holes: Ess = Essertines; Tre = Treycovagnes; Val = Valempoulières. Coordinates (in km) are according to the national Swiss geographical coordinate system. Gray thin lines represent the seismic grid. Modified from Sommaruga (1995).

land belt and could therefore be expected to be more evolved than the Jura folds. Molasse folds, however, represent typically early-stage buckle folds and their Triassic cores seem to be filled with well-organized evaporite duplexes (Fig. 12). The most obvious reason for this apparent contradiction seems to be the load of the Tertiary sediments increasing from north to south, which prevented the Molasse basin buckle folds from evolving further into thrust-related folds. With future deformation and concomitant erosion of the Tertiary wedge sediments, Molasse basin anticlines could evolve into Jura folds. The present day taper of the Alpine front would probably favor a back-stepping thrust sequence with the most frontal thrust emerging close to the Molasse Basin/Haute Chaîne Jura border (Mugnier & Ménard, 1986).

Inversion tectonic structures e.g., partly inverted Permo-Carboniferous (half-) grabens have been described in the westernmost Jura based on the deep seismic ECORS reflection profiles (Guellec et al., 1990). In the western Molasse Basin, especially the Geneva area, recent work based on seismic data (Gorin et al., 1993; Signer & Gorin, 1995) highlights the presence of NE–SW and NW–SE trending Permo-Carboniferous lineaments which would have been reactivated several times until the present day. In the eastern Jura, some minor normal faults have been identified at the border between thrust nucleation and inherited structures e.g., Paleozoic graben system or Oligocene N–S oriented normal faults related to the Rhine-Bresse graben system (Laubscher, 1985; 1986; Naef & Diebold, 1990; Noack, 1995). Total short-

ening within the Jura cover, however, is in excess of 25 km and cannot be explained with the weak shortening associated with all these apparently late (Pliocene?) inversion structures. Seismic data interpreted in this work do not present any positive evidence for inversion of Permo-Carboniferous grabens or for thrust fault nucleation related to inhomogeneities in the basement.

North–south oriented tear faults in the North Alpine foreland are interpreted by many authors as inherited features related to the Oligocene opening of the Rhine-Bresse Graben system (Elmohandes, 1981; Illies, 1981; Laubscher, 1973a, 1992; Bergerat, 1987). During Miocene folding and thrusting of the Jura, preexisting faults and joints represented major anisotropies within the Mesozoic cover. They were reactivated during and after folding and played an important role in localizing bends and discontinuities in folds during shortening. The N–S strike of preexisting faults and joints thereby reactivated sinistral transcurrent deformation, compatible with the overall N-to-NW-directed Alpine push (Laubscher, 1972). However, seismic lines in the central Jura do not support, in general, arguments in favor or against inherited faults.

A common feature of foreland fold-and-thrust belts (e.g., Melville Island, Appalachian Plateau, Alberta and British Columbia Rocky Mountains) is the presence of a weak basal décollement surface or zone (salt, other evaporites or shales), which dips towards the hinterland and below which relatively little deformation occurs (Chapple, 1978; Davis & Engelder, 1985). Many fold-and-thrust belts around the world have developed above a weak basal layer. A comparison of these belts has allowed some authors e.g., Bally et al., (1966), Davis and Engelder (1985; 1987) to characterize these compressional terranes as broad belts with a low-angle cross-sectional taper, laterally continuous symmetric folds, broad synclines, anticlinal salt flow and forward- as well as backward-verging folds and thrusts.

The critical taper is the cross-sectional wedge profile maintained when an entire thrust belt is on the verge of horizontal compressive failure. The magnitude of the angle between surface topography and the décollement surface of the critical taper is governed by the relative magnitudes of the frictional resistance along the base and the compressive strength of the wedge material (Dahlen, 1990). The critical angle is therefore the sum of the angles of the décollement dip, which is towards the hinterland, and the topographic slope towards the foreland (Chapple, 1978; Davis & Engelder, 1985; Dahlen, 1990). Foreland fold-and-thrust belts riding above salt décollements typically have extremely low critical taper angles of less than 1° (Dahlen et al., 1984; Davis & Engelder, 1985; 1987) and in these cases topographic slopes may be virtually absent. In such a low angle taper, internal deformation of the wedge may take place by symmetric foreland- or hinterland-vergent thrusts. This is in contrast to higher angle tapers (commonly in excess of 8°), where a predominance of shallow foreland vergent thrusts is both predicted and observed (Davis & Engelder, 1985; Dahlen, 1990). Recently Philippe (1995), and Phillipe et al., (1996) calculated a critical taper angle of 3.4° for the Jura fold-and-thrust belt, based on an angle of 1.6° for the topography and 1.8° for the basement. This is in good agreement with results herein, since an angle of 1–2° for the basal décollement is observed on the top of basement map from the central Jura (Fig. 20). In the southwestern area of the Jura belt evaporites lack, therefore, the critical taper increases considerably and thrust sheets are piled up on each other (Philippe et al., 1996). However, the topographic slope, when considered from the toe of the Jura to the crest of the Alps, does show a conspicuous hinter land-dipping portion located at the transition from the Jura to the Molasse Basin (Fig. 3). This hinterland-dipping slope can be explained by the important Plio-Pleistocene erosion as well as glacial erosion during Pleistocene time in the Molasse Basin. Deformation to the southeast of this line is considerably less than in the Jura itself, apparently in contradiction with a simple foreland fold-and-thrust belt wedge model which would predict increasing deformation intensity from foreland to hinterland. Perhaps the most outstanding feature of the Jura arc is its position at the outward rather than the inward side of the foreland basin, which is directly related to the Triassic evaporite distribution.

Jura folding and thrusting is younger than late Middle Miocene (Laubscher, 1987; Bolliger et al., 1993; Kälin, 1993), since Serravallian lacustrine Molasse series are clearly involved in folding and thrusting. Locally, however, some intra-Molasse unconformities and fault-scarp breccias indicate earlier syn-depositional tectonics which seem to be more pronounced at the southwestern end (Deville et al., 1994) of the Jura than in central and eastern parts. No unconformities other than the basal foredeep unconformity could be detected on seismic lines from the central Jura, and Molasse Basin. Molasse internal structures are poorly imaged on the presently available seismic lines, however. The deformation of the Jura cover halted subsidence of the Molasse basin and controlled its uplift.

In conclusion, the interpretation of more than 1500 km of seismic reflection lines across all tectonic units of the Jura and Molasse Basin has not revealed any obvious examples where cover structures can be related to observable, reliable deformation in the underlying basement. No deformation features are observed in the basement. Instead the overlying Triassic Unit 2 layers are deformed, showing mainly evaporite swells. Any irregularities which might exist in the top of the basement are small compared with the thickness of Triassic Unit 2. This leads to the conclusion that the Jura and Molasse Basin cover has been deformed over a main décollement zone located in Triassic Unit 2. This conclusion corresponds to the

'Fernschub theory' formulated by Buxtorf (1916). Nevertheless the link between the Jura fold-and-thrust belt and the Alps chain remains debatable (Fig. 4). Authors have proposed various hypotheses based on field work, fission-track data, balancing concepts and recently refraction or reflection seismic data; see reviews by Burkhard (1990) and Laubscher (1992). One hypothesis connects the Jura basal thrust to the basal Helvetic thrust and implies that uplift of the external crystalline massifs would post-date the Jura thrusting (Laubscher, 1973b). The internal deformation within the external crystalline massifs would be explained by vertically extending pure shear (Marquer, 1990) or by differential isostatic uplift (Neugebauer et al., 1980). Another hypothesis, first expressed by Boyer and Elliott (1982), states that the Jura basal thrust continues beneath the Molasse Basin and then roots in the frontal part of the external crystalline massifs and uplift of the latter is coeval with folding and thrusting deformation in the Jura. This hypothesis is the most widely accepted today.

Acknowledgements

This work has been made possible thanks to the following companies which have kindly given access to the seismic lines: British Petroleum Exploration Operating Company (Middlesex, U.K.), Forces Motrices Neuchâteloises S.A. (Switzerland), Geological Museum of Canton de Vaud at Lausanne (Switzerland), Shell International Exploration and Production B.V. (Netherlands). I would like to thank them for their confidence. I am indebted to A.W. Bally, M. Burkhard, G. Gorin, J. Mosar, D.G. Roberts, J.-P. Schaer and G. Schönborn for constructive remarks and stimulating discussion. Special thanks to P.A. Ziegler and an anonymous reviewer for helpful comments and suggestions. This study, which represents part of a PhD thesis, has been financially supported by the Swiss National Foundation (Grant No 21-37366.93) and by Neuchâtel University.

References

Aubert, D. (1945). Le Jura et la tectonique d'écoulement. *Mém. soc. vaudoise des sci. nat., 8*, 217–236.

Bachmann, G. H., Müller, M., & Weggen, K. (1987). Evolution of the Molasse Basin (Germany, Switzerland). *Tectonophysics, 137*, 77–92.

Bally, A. W., Gordy, P. L., & Stewart, G. A. (1966). Structure, seismic data and orogenic evolution of southern Canadian Rocky Mountains. *Bull. Can. Petrol. Geol., 14*, 337–381.

Bergerat, F. (1987). Paléo-champs de contrainte tertiaires dans la plateforme européenne au front de l'orogène alpin. *Bull. Soc. géol. France, 8*, 611–620.

Bitterli, P. (1972). Erdölgeologische Forschungen im Jura. *Bull. Ver. Schweizer. Petrol-Geol. u. Ing., 39*, 13–28.

Bitterli, T. (1992). *Die Anwendung der tektonischen Materialbilanz im östlichen Faltenjura*. PhD thesis, University of Basel, Switzerland.

Bolliger, T., Engesser, B., & Weidmann, M. (1993). Première découverte de mammifères pliocènes dans le Jura neuchâtelois. *Eclogae geol. Helv., 86*, 1031–1068.

Boyer, S. E., & Elliott, D. (1982). Thrust systems. *Amer. Ass. Petrol. Geol. Bull., 66*, 1196–1230.

BRGM(1964). In *Mouthe. Carte géologoqie détaillée de la France* 1:50,000, feuille 583. Service de la Carte géologique de la France.

Burkhard, M. (1990). Aspects of the large scale Miocene deformation in the most external part of the Swiss Alps (Subalpine Molasse to Jura fold belt). *Eclogae geol. Helv., 83*, 559–583.

Burkhard, M., Atteia, O., Sommaruga, A., Gogniat, S., & Evard, D. (1998). Tectonique et hydrogéologie dans le Jura Neuchâtelois. *Eclogae geol. Helv., 91*, 177–183.

Burkhard M., & Sommaruga A. (1998). Evolution of the western Swiss Molasse basin: structural relations with the Alps and the Jura belt. In Mascle A. (Ed.), *Foreland Basins of the western Alpine Thrust Belts*, pp. 279–298. London: Geological Society Special Publication

Buxtorf, A. (1916). Prognosen und Befunde beim Hauensteinbasis- und Grencherberg-tunnel und die Bedeutung der letzteren für die Geologie des Juragebirges. *Verh, Naturforsch. Ges. Basel, 27*, 184–205.

Chapple, W. M. (1978). Mechanics of thin-skinned fold-and-thrust belts. *Geol. Soc. Amer., Bull., 89*, 1189–1198.

Coward, M., & Stewart, S. (1995). Salt-influenced structures in the Mesozoic-Tertiary cover of the southern North Sea, U.K. In (pp. 229–250). M.P.A. Jackson, D.G. Roberts, S. Snelson (Eds.), *Salt tectonics; a global perspective*, Vol. 65. American Association of Petroleum Geologists Memoir.

Dahlen, F. A. (1990). Critical taper model of fold-and-thrust belts and accretionary wedges. *Ann. Rev. Earth Planet. Sci., 18*, 55–99.

Dahlen, F. A., Suppe, J., & Davis, D. M. (1984). Mechanics of fold-and-thrust belts and accretionary wedges (continued): Cohesive Coulomb theory. *J. Geophys. Res., 88*, 1153–1172.

Dahlstrom, C. D. A. (1970). Structural geology in the eastern margin of the Canadian Rocky Mountains. *Bull. Can. Petrol. Geol., 18*, 332–406.

Davis, D. M., & Engelder, T. (1985). The role of salt in fold-and-thrust belts. *Tectonophysics, 119*, 67–88.

Davis, D. M., & Engelder, T. (1987). Thin-skinned deformation over salt. In I. Lerche, J. J. O'Brien (Eds.), *Dynamical Geology of Salt and Related Structures* (pp. 301–337). Academic Press Inc.

De Margerie, E. (1922). In *Le Jura. Première Partie: Bibliographie sommaire du Jura français et suisse (orographe, tectonique et morphologie)*. Paris: Ministère des Travaux Publics.

Debrand-Passard, S., & Courbouleix, S. (1984). In *Synthèse géologique de Sud-Est de la France*. Atlas. Orléans: BRGM.

Deville, E., Blanc, E., Tardy, M., Beck, E., Cousin, M., & Ménard, G. (1994). Thrust propagation and syntectonic sedimentation in the Savoy Tertiary Molasse basin (Alpine Foreland). In (pp. 269–280). A. Mascle (Ed.), *Hydrocarbon and petroleum geology of France*, Vol. 4. Europ. Assoc. Petrol. Geol. Spec. Publ.

Dickinson, W. R. (1974). Plate tectonics and sedimentation. In (pp. 1–27). W.R. Dickinson (Ed.), *Tectonics and Sedimentation*, Vol. 22. Special Publication of the Society of economic Paleontologists and Mineralogists.

Dixon, J. M., & Liu, S. (1992). Centrifuge modelling of the propagation of thrust faults. In K. R. McClay (Ed.), *Thrust tectonics* (pp. 53–68). Chapman & Hall.

Elmohandes, S. E. (1981). The central European Graben system: Rifting imitated by clay modelling. *Tectonophysics, 73*, 69–78.

Gorin, G. E., Signer, C., & Amberger, G. (1993). Structural configuration of the western Swiss Molasse Basin as defined by reflection seismic data. *Eclogae geol. Helv., 86*, 693–716.

Guellec, S., Mugnier, J. L., Tardy, M., & Roure, F. (1990). Neogene evolution of the western Alpined foreland in the light of ECORS data and balanced cross sections. In (pp. 165–184). F. Roure, P.

Heitzmann, R. Polino (Eds.), *Deep structure of the Alps*. Vol. 1. Mém. Soc. géol. suisse.

Harrison, J. C. (1995). Melville Island's salt-based fold belt, Arctic Canada. *Geol. Surv. Canada, Bull., 472*, 1–331.

Harrison, J. C., & Bally, A. W. (1988). Cross-sections of the Parry Islands Fold Belt on Melville Island, Canadian Arctic Islands: implications for the timing and kinematic history of some thin-skinned décollement systems. *Bull. Can. Petrol. Geol., 36*, 311–332.

Heim, A. (1915). Die horizontalen Transversalverschiebungen im Juragebirge. Geol. Nachlese Nr.22. *V. Natf. Ges. Zürich, 60*, 597–610.

Heim, A. (1921). In *Geologie der Schweiz, Band 1 Molasseland und Juragebirge* (pp. 704). *Vol. Band 1: Molasseland und Juragebirge*. Tauchniz.

Homewood, P., Rigassi, D., & Weidmann, M. (1989). Le bassin molassique Suisse. In Assoc. Sédim. Française (Ed.), *Dynamique et méthodes d'étude des bassins sédimentaires* (pp. 299–314). Technip.

Illies, J. H. (1981). Mechanism of graben transformation. *Tectonophysics, 73*, 249–266.

Jackson, M. P. A., & Vendeville, B. C. (1994). Initiation of salt diapirism by regional extension; global setting, structural style and mechanical models. University of Texas, Bureau of Economic Geology, Texas, USA: Austin.

Kälin D. (1993). Stratigraphie und Säugetierfaunen der oberen Süsswassermolasse der Nordwestschweiz. PhD thesis, ETH Zürich, Switzerland

Laubscher, H. P. (1961). Die Fernschubhypothese der Jurafaltung. *Eclogae geol. Helv., 54*, 221–280.

Laubscher, H. P. (1965). Ein kinematisches Modell der Jurafaltung. *Eclogae geol. Helv., 58*, 232–318.

Laubscher, H. P. (1972). Some overall aspects of Jura dynamics. *Amer. J. Sci., 272*, 293–304.

Laubscher, H. P. (1973). Faltenjura und Rheingraben: zwei Grossstrukturen stossen zusammen. *Jber. Mitt. oberrh. geol. Ver., N.F., 55*, 145–158.

Laubscher, H. P. (1973). Jura Mountains. In K. A. De Jong, R. Scholten (Eds.), *Gravity and Tectonics* (pp. 217–227). Wiley.

Laubscher, H. P. (1977). Fold development in the Jura. *Tectonophysics, 37*, 337–362.

Laubscher, H. P. (1985). The eastern Jura: relations between thin-skinned and basement tectonics, local and regional, NTB85-53. Baden: Nagra.

Laubscher, H. P. (1986). The eastern Jura: relations between thin-skinned and basement tectonics, local and regional. *Geol. Rdsch., 75*, 535–553.

Laubscher, H. P. (1987). Die tektonische Entwicklung der Nordschweiz. *Eclogae geol. Helv., 80*, 287–303.

Laubscher, H. P. (1992). Jura kinematics and the Molasse basin. *Eclogae geol. Helv., 85*, 653–676.

Letouzey, J., Colletta, B., Vially, R., & Chermette, J. C. (1995). Evolution of salt-related structures in compressional settings. In (pp. 41–60). M. P. A. Jackson, D. G. Roberts, S. Snelson (Eds.), *Salt tectonics; a global perspective*. Vol. 65. American Association of Petroleum Geologists Memoir.

Marquer, D. (1990). Structure et déformation alpine dans les granites hercyniens du massif du Gothard (Alpes centrales suisses). *Eclogae geol. Helv., 83*, 77–97.

McClay, K. R. (1992). In *Thrust tectonics* (pp. 447). Chapman & Hall.

Meia, J. (1987). Derniers regards sur la Mine d'asphalte de La Presta (Val-de-Travers, Jura neuchâtelois, Suisse). *Bull. Ver. Schweizer. Petrol.-Geol. u. Ing., 53*, 47–56.

Mitchum, R. M., & Vail, P. R. (1977). Seismic stratigraphic interpretation procedure. In (pp. 135–144). C.E. Payton (Ed.), *Seismic stratigraphy – Applications to hydrocarbon exploration*. Vol. Memoir 26. American Association of Petroleum Geologists.

Mitra, S. (1986). Duplex structures and imbricate thrust systems: geometry, structural position, and hydrocarbon potential. *Amer. Ass. Petrol. Geol. Bull., 70*, 1087–1112.

Mugnier, J. L., & Ménard, G. (1986). Le développement du bassin molassique suisse et l'évolution des Alpes externes: un modèle cinématique. *Bull. Cent. Rech. Explor.-Prod. Elf-Aquitaine, 10*, 167–180.

Naef, H., & Diebold, P. (1990). Interprétation géologique de la sismique réflexion. *Cédra informe, 2*, 16–28.

Neugebauer, H. J., Brötz, R., & Rybach, L. (1980). Recent crustal uplift and the present stress field in the Alps along the Swiss Geotraverse Basel Chiasso. *Eclogae geol. Helv., 73*, 489–500.

Noack, T. (1995). Thrust development in the eastern Jura Mountains related to pre-existing extensional structures. *Tectonophysics, 252*, 419–431.

Otto, S. (1994). In *Bresse-Valence Basin & Jura foldbelt*. Geneva, Switzerland: Petroconsultants.

Palmer, A. R. (1983). Geologic Time Scale. In *Decade of the North American Geology*. Boulder, Colorado: Geological Society of America.

Pavoni, N. (1961). Faltung durch Horizontalverschiebung. *Eclogae geol. Helv., 54*, 515–534.

Pfiffner, O. A. (1994). Structure and evolution of the Swiss Molasse Basin in the transect Aar Massif-Bern-Central Jura. *Géologie Alpine, 4*, 85.

Pfiffner, O. A., Erard, P. F., & Stäuble, M. (1997). Two cross sections through the Swiss Molasse Basin (line E4–E6, W1, W7–W10). In A.O. Pfiffner, P. Lehner, P. Heitzmann, S. Müller, A. Steck (Eds.), *Deep structure of the Swiss Alps, results of NRP 20* (pp. 64–72). Birkhäuser Verlag.

Philippe, Y. (1994). Transfer Zone in the southern Jura Thrust Belt (eastern France): Geometry, development and comparison with analogue modelling experiments. In (pp. 327–346). A. Mascle (Ed.), *Hydrocarbon and petroleum geology of France*, Vol. 4. Europ. Assoc. Petrol. Geol. Spec. Publ.

Philippe Y. (1995). Rampes latérales et zones de transfert dans les chaînes plissées: géométrie, conditions de formation et pièges structuraux associés. PhD thesis, University of Chambéry, Savoie, France

Philippe, Y., Coletta, B., Deville, E., & Mascle, A. (1996). The Jura fold-and-thrust belt: a kinematic model based on map-balancing. In (pp. 235–261). P. A. Ziegler, F. Horvath (Eds.), *Peri-Tethys Memoir 2: Structure and Prospects of Alpine Basins and Forelands*, Vol. vol. 170. Mémoire du Muséum national d'Histoire naturelle.

Price, R. A. (1973). Large-scale gravitational flow of supracrustal rocks, southern Canadian Rockies. In K. A. De Jong, R. Scholten (Eds.), *Gravity and tectonics* (pp. 491–502). Wiley and Sons.

Rigassi, D. A. (1962). A propos de la tectonique du Risoux (Jura vaudois et franc-comtois). *Bull. Ver. Schweizer. Petrol.-Geol. u. Ing., 29*, 39–50.

Rodgers, J. (1990). Fold-and-thrust belts in sedimentary rocks, Part 1: typical examples. *Amer. J. Sci., 290*, 321–359.

Schnegg, P-A., & Sommaruga, A. (1995). Constraining seismic parameters with a controlled-source audio magnetotelluric method (CSAMT). *Geophys. J. Int., 122*, 152–160.

Signer, C., & Gorin, G. E. (1995). New geological observations between the Jura and the Alps in the Geneva area, as derived from reflection seismic data. *Eclogae geol. Helv., 88*, 235–265.

Sommaruga, A. (1995). Tectonics of the central Jura and the Molasse Basin. New insights from the interpretation of seismic reflection data. *Bull. Soc. neuchâtel. Sci. Nat., 118*, 95–108.

Sommaruga, A. (1997). Geology of the central Jura and the Molasse Basin: new insight into an evaporite-based foreland fold and thrust belt. *Mém. Soc. neuchâtel. Sci. Nat., XII*, 1–176.

Trümpy, R. (1980). In *Geology of Switzerland—a guide-book. Part A: An outline of the geology of Switzerland, Part B: Geological excursions*. Basel, New York, Wepf.

Trusheim, F. (1960). Mechanism of salt migration in northern Germany. *Amer. Ass. Petrol. Geol. Bull., 44*, 1519–1540.

Twiss, R. J., & Moores, E. M. (1992). In *Structural Geology*. New York: W. H. Freeman and Company.

Vendeville, B. C., & Jackson, M. P. A. (1992). The fall of diapirs during thin-skinned extension. *Marine Petroleum Geol., 9*, 354-371.

Vendeville, B. C., & Jackson, M. P. A. (1992). The rise of diapirs during thin-skinned extension. *Marine Petroleum Geol., 9*, 331-353.

Wegmann, E. (1963). Le Jura plissé dans la perspective des études sur le comportement des socles. In (pp. 99 104). Soc. Geol. France (Ed.), *Livre Mém. Prof. P. Fallot*, Vol. Mém. hors-séie 1.

Winnock, E. (1961). Résultats géologiques du forage Risoux 1. *Bull. Ver. Schweizer. Petrol.-Geol. u. Ing., 28*, 17–26.

Winnock, E., Barthe, A., & Gottis, C. (1967). Résultats des forages pétroliers français effectués dans l région voisine de la frontière suisse. *Bull. Ver. Schweizer. Petrol.-Geol. u. Ing., 33*, 7–22.

Ziegler, P. A. (1982). In *Geological Atlas of Western and Central Europe*. The Hague: Shell Internationale Petroleum Maatschappij BV.

Ziegler, P. A. (1990). In *Geological Atlas of Western and Central Europe*. Netherlands, Shell Internationale Petroleum Maatschappij BV: Mijdrecht.

Ziegler, P. A., Schmid, S. M., Pfiffner, A., & Schönborn, G. (1996). Structure and evolution of the Central Alps and their northern and southern foreland basins. In (pp. 211-233). P. A. Ziegler, F. Horvath (Eds.), *Peri Tethys Memoir 2: Structure and Prospects of Alpine Basins and Forelands*, Vol. 170. Mémoire du Muséum national d'Historie naturelle.

Zweidler D. (1985). Genèse des gisements d'asphalte de la Pierre Jaune de Neuchâtel et des calcaires urgoniens du Jura (Jura neuchâtelois et nord-vaudois, Suisse). PhD thesis, University of Neuchâtel, Switzerland